Check for updates

Leaf isoprene and monoterpene emissions vary with fast-slow carbon economics strategies in central Amazon woody species

Michelle Robin[1,2]*, Eliane Gomes Alves[1,3], Tyeen C. Taylor[4,5], Débora Pinheiro Oliveira[3], Sérgio Duvoisin Jr.[6], José Francisco C. Gonçalves[7], Jochen Schöngart[7], Florian Wittmann[8], Maria T. F. Piedade[7], Susan Trumbore[1] and Juliana Schietti[2,9]

[1]Department of Biogeochemical Processes, Max Planck Institute for Biogeochemistry, Jena, Germany, [2]Post-Graduation Program in Ecology, National Institute of Amazonian Research, Manaus, Brazil, [3]Post-Graduation Program in Climate and Environment, National Institute of Amazonian Research, Manaus, Brazil, [4]Department of Civil and Environmental Engineering, University of Michigan, Ann Arbor, MI, United States, [5]Biology Department, University of Miami, Coral Gables, FL, United States, [6]Department of Chemistry, University of the State of Amazonas, Manaus, Brazil, [7]Coordination of Environmental Dynamics, National Institute of Amazonian Research, Manaus, Brazil, [8]Department of Wetland Ecology, Karlsruhe Institute of Technology, Rastatt, Germany, [9]Department of Biology, Federal University of Amazonas, Manaus, Brazil

Plant responses to stress, inter-organismal signaling, and atmospheric chemistry are significantly influenced by leaf volatile isoprenoid (VI) emissions (e.g., isoprene and monoterpenes). Despite their critical roles in ecology and the atmosphere, we have little understanding of whether and how VI emissions vary with axes of plant functional variation. Understanding these relationships is particularly important in tropical forests, which emit more VIs into the atmosphere than any other biome, and where high species diversity necessitates the imputation of plant traits based on functional and evolutionary relationships. Here, we investigated how VI emissions varied with functional trait axes of fast-slow carbon economics strategies (CES) in Central Amazon Forest woody species. We measured leaf-level isoprene and monoterpene emission capacity (E_c; emission measured under standard conditions of photosynthetically active radiation of 1000 µmol m^{-2} s^{-1} and leaf temperature of 30 ˚C), and 12 leaf and four stem functional traits for 91 trees from 31 species of angiosperm distributed across different vegetation types: non-flooded upland, white sand, and ancient non-flooded river terrace forests. Principal component analysis (PCA) of functional traits revealed two partially independent main axes of CES: a first axis of leaf strategies and a second of mixed leaf/stem strategies. The capacity to emit monoterpenes was observed in 27 species, and monoterpene emitters occupied the whole range of fast-slow strategies, but magnitudes of monoterpene E_c increased toward faster leaves. The capacity to emit isoprene was observed in 14 species, and isoprene emitters tended to be positioned toward slower leaf/stem strategies, with magnitudes of isoprene E_c also increasing toward slower leaves/stems. Our results highlight the importance of understanding leaf-level emissions to accurately estimate VI fluxes and provide a holistic view of emissions within CES on different organ-system levels. This shows a direction for improving current modeling estimates, which have

simplified plant functional type representations and are poorly developed for compounds other than isoprene in the tropics. A more mechanistic representation of plant functional types based on forest functional compositions can reduce modeling emission uncertainties and contribute to understanding the roles of VIs within forest-atmosphere interactions, atmospheric chemistry, and the carbon cycle.

1 Introduction

Isoprenoids are the most abundant and chemically diverse group of secondary plant metabolites with important roles in primary and secondary metabolism (Thulasiram et al., 2007). They regulate plant physiological functions, protect against biotic and abiotic stress, take part in plant-plant signaling, and interfere in plant-herbivore interactions (Singsaas et al., 1997; Pichersky and Gershenzon, 2002; Gershenzon and Dudareva, 2007; Laothawornkitkul et al., 2008; Fineschi and Loreto, 2012; Xiao et al., 2012; Pollastri et al., 2014, 2019; Monson et al., 2021; Dani et al., 2022). Isoprene and monoterpenes are highly emitted volatile isoprenoids (VIs), accounting for the largest share of global biogenic volatile organic compound (BVOC) emissions (Guenther et al., 2006, 2012). Upon entering the atmosphere, these compounds have major influence over atmospheric chemical and physical processes, including secondary organic aerosol formation, which can affect the radiative balance of the Earth (Pöschl et al., 2010; Kulmala et al., 2013).

Tropical forests contribute to around 80% of global BVOC fluxes (Guenther et al., 2012), and the Amazon Forest, with its high plant biomass and species diversity (Cardoso et al., 2017), is considered the greatest and most diverse source of emissions. However, estimating VI fluxes from this forest is challenging due to an insufficient understanding of physiological and ecological controls on forest emissions, and the forest's huge diversity of plant species and functional strategies (Alves et al., 2016, 2018; Taylor et al., 2018, 2021). Even though the existing knowledge on the ecophysiology of VI emissions has considerably increased over the last two decades (Morfopoulos et al., 2013; Sharkey and Monson, 2017; Alves et al., 2018; Taylor et al., 2018, 2021; Yáñez-Serrano et al., 2020; Monson et al., 2021; Gomes Alves et al., 2022, 2023; Robin et al., 2024), we still do not know exactly how isoprene and monoterpene emissions vary with plant functional strategies (Sardans et al., 2010; Harrison et al., 2013; Dani et al., 2014; Llusia et al., 2014; Fernández-Martínez et al., 2018), particularly in Amazonian woody species.

Isoprene (C_5H_8) emissions are light and temperature-dependent, and primarily produced from recently assimilated photosynthetic carbon (*de novo* synthesis) (Sharkey and Monson, 2017). Isoprene is mostly known for its role in thermoprotection (Singsaas et al., 1997; Pollastri et al., 2014, 2019), which has been attributed to increased thylakoid membrane stability (Velikova et al., 2011; Harvey et al., 2015) or direct/indirect antioxidant properties (Morfopoulos et al., 2013, 2014; Rodrigues et al., 2020; Velikova, 2008). More recently, multi-omic studies have demonstrated that the capacity to emit isoprene is associated with changes in gene expression and transcription factors that participate in the production of various growth and defense-related compounds (Behnke et al., 2010; Harvey and Sharkey, 2016; Lantz et al., 2019; Zuo et al., 2019; Frank et al., 2021; Monson et al., 2021; Dani et al., 2022; Srikanth et al., 2024; Weraduwage et al., 2024). These studies propose that the capacity to emit isoprene is a trait that mediates photosynthetic resource supply and metabolite demands in the face of climate stress (Monson et al., 2021).

Monoterpenes ($C_{10}H_{16}$) have been more frequently associated with slow, constitutive emissions from storage pools formed inside specialized structures, and with stronger stress-induced emissions upon breakage of these pools (e.g., insect attacks) (Arneth and Niinemets, 2010; Niinemets et al., 2013; Rasulov et al., 2019; Nagalingam et al., 2023). Monoterpene emissions exert diverse chemical signaling roles in direct and indirect defense against herbivores and plant communication (Gershenzon and Dudareva, 2007; Fineschi and Loreto, 2012; Xiao et al., 2012). However, many studies have reported leaf-level light-dependent *de novo* monoterpene emissions, especially in tropical forests, and a role in oxidative stress protection similar to isoprene has been proposed for these compounds (Kuhn et al., 2004; Jardine et al., 2015, 2017, 2020; Gomes Alves et al., 2022; Bourtsoukidis et al., 2024). While VIs are not essential for plant growth and survival (Owen and Peñuelas, 2005), the capacity to produce these compounds can be a major advantage for plant survival since they confer protection against many biotic and abiotic stressors (Loreto and Schnitzler,

2010; Fineschi and Loreto, 2012; Monson et al., 2021; Srikanth et al., 2024). Yet, VI production demands resources (carbon) that could otherwise be allocated toward plant respiration and growth (Delwiche and Sharkey, 1993; Affek and Yakir, 2003; Loreto et al., 2004; Huang et al., 2017; Lehmanski et al., 2024). Similarly, higher production of *de novo*-emitted compounds would be generally associated with a greater reallocation of photosynthetic carbon to VI production (Delwiche and Sharkey, 1993; Loreto et al., 1996).

Isoprene and light-dependent monoterpenes are both produced in the chloroplastic methyl-erythritol 4-phosphate (MEP) pathway, having dimethylallyl pyrophosphate (DMAPP) as a common precursor (Zhao et al., 2013). Monoterpenes not only contain double the amount of carbon atoms per molecule compared to isoprene, but also present a higher complexity in chemical structure (e.g., acyclic, monocyclic, bicyclic) (Thulasiram et al., 2007), and are produced one chemical reaction step later than that of isoprene (Zhao et al., 2013). This suggests that monoterpenes incur higher construction costs on both mass and energy bases. However, the affinity of isoprene synthase for DMAPP is much lower (Michaelis-Menten coefficient, K_m = 0.3 - 2.45 mM) than that of geranyl pyrophosphate synthase (GPS) for DMAPP (K_m = 0.014 - 0.037 mM) and that of monoterpene synthases for geranyl pyrophosphate (GPP) synthesized by GPS (K_m = 0.006 - 0.009 mM) (Harrison et al., 2013). Hence, even though isoprene is produced earlier in the MEP pathway, DMAPP is more easily converted to monoterpenes than to isoprene (Harrison et al., 2013). This means that a higher affinity of monoterpene synthases for DMAPP might counteract a possible lower carbon cost bias in favor of isoprene production.

Still, VIs share the same biochemical pathway of essential isoprenoids like plant hormones (abscisic acid and gibberellins) and photosynthetic pigments (chlorophyll and carotenoids) (Laule et al., 2003), and it has been suggested that VI emissions are "opportunistic" in the sense that they make use of the available DMAPP surplus when the demands for essential isoprenoid production are met (Owen and Peñuelas, 2005). However, some studies have also demonstrated that, under abiotic stress, the amount of photosynthetic carbon loss with isoprene and light-dependent monoterpene emissions can account for up to 20 and 7.4% of photosynthesis, respectively (Bamberger et al., 2017; Robin et al., in prep.). Such high percentages of photosynthetic carbon loss in stress conditions suggest that plants can also actively allocate carbon toward VI emissions despite metabolite demands downstream of the MEP pathway, which emphasizes the physiological importance of these compounds.

Therefore, a balance between the benefits for plant defense - and survival - and the associated carbon costs of isoprene and light-dependent monoterpene production possibly illustrates an ecological tradeoff that may allow evaluating their emissions from a functional ecology perspective. Functional ecology classifies and identifies organisms by sets of measurable characteristics (i.e., functional traits) that impact individual performance (e.g., growth, development, defense, survival, and reproduction) (Violle et al., 2007). Resource allocation strategies describe how plants balance growth and differentiation to optimize fitness through correlations in traits related to resource acquisition, processing,

and conservation. These strategies ultimately inform the conceptual framework of carbon economics strategies (CES) (Reich, 2014), which explains how plants allocate carbon to various functions to maximize growth or survival. Within CES, the leaf economics spectrum captures tradeoffs in leaf traits related to carbon acquisition and conservation, classifying species from fast-growing, acquisitive: ones with lower leaf mass per area (LMA), higher nitrogen and phosphorus per dry mass (N_{mass} and P_{mass}), and higher photosynthetic capacities (A_{max}) - traits that enable faster returns (i.e. higher growth rates) upon assimilated carbon; to slow-growing, conservative species: with higher LMA, lower N_{mass} and P_{mass}, and lower A_{max} - providing slower returns but greater tissue longevity (i.e. lower mortality rates) (Wright et al., 2004). Similarly, the wood economics spectrum encompasses variation in stem traits, where slow-growing species show dense, durable wood that supports long-term survival; in contrast with fast-growing species that show lighter, less dense wood that favors rapid growth (Chave et al., 2009).

Harrison et al. (2013) showed that isoprene emission rates increase with specific leaf area (SLA), short leaf lifespan, and A_{max}, and decrease with increased constitutive monoterpene emissions. This led to an association between isoprene and faster-growth strategies, and the hypothesis that monoterpene emissions would be associated with slower-growth strategies due to their comparably higher production costs and longer-term protective role (as these are storable compounds) against herbivores - although isoprene has been shown as involved in herbivore deterrence as well (Visakorpi et al., 2018; Pollastri et al., 2021). Likewise, Dani et al. (2014) proposed that deciduous trees (i.e., faster leaves) would be high isoprene emitters, but that evergreen trees (i.e., slower leaves) would be high monoterpene emitters - though this construct may be biased by the rarity of evergreen angiosperms in the temperate zone. Although these studies have attempted to position changes in VI emissions within CES, they are generally biased toward temperate forest species due to the higher availability of data for this biome. Moreover, studies focusing on tropical woody species are few and unclear (Sardans et al., 2010; Llusia et al., 2014) and relationships between the capacity to emit and the magnitude of VI emissions and CES in Central Amazon Forest woody species have not yet been evaluated.

Here we investigated how leaf-level VI emission capacity (E_c = emission measured at standard conditions of photosynthetically active radiation of 1000 µmol m^{-2} s^{-1} and leaf temperature of 30 ˚C) varies with fast-slow CES strategy axes derived from correlations between 16 functional traits (12 leaf traits and four stem traits) measured *in situ* for 91 trees from 31 species of angiosperm in a central Amazon site. Considering the positive impacts of VI emissions on plant defense and survival, and their associated carbon production costs, we hypothesized that (H1) both the capacity to emit and the magnitude of VI E_c vary with CES and are either (H1a) associated with faster strategies due to higher photosynthetic rates required to cover carbon demands of emissions or (H1b) associated with slower strategies where higher carbon demands from emissions are compensated by greater leaf longevity; and that (H2) both the capacity to emit and the

magnitude of isoprene and monoterpene E_c vary simultaneously with CES in the sense that either (H2a) the capacity to emit isoprene and monoterpenes or the magnitude of their E_c are mutually exclusive, as the increasing carbon cost of one must be compensated by a decreasing cost of the other, or (H2b) the capacity to emit isoprene and monoterpenes or the magnitude of their E_c are positively associated due to their complementary roles in oxidative stress protection.

2 Materials and methods

2.1 Study site

This study was conducted at the Amazon Tall Tower Observatory (ATTO) and PELD-MAUA (PELD is the acronym in Portuguese for Long Term Ecological Research Project) experimental plots. Plots are located in the central Amazon region, at the Uatumã Sustainable Development Reserve (USDR), about 150 km northeast of the city of Manaus (S 02 08.9° W 059 00.2°) (Supplementary Figure S1). The climate is tropical humid, with a mean annual temperature of 26.7 °C and precipitation of 2376 mm, being characterized by a pronounced rainy season from November-May and a drier season from June-October (Andreae et al., 2015). The reserve covers 424,430 ha with a mosaic of non-flooded upland (locally called *terra firme*), white sands, and ancient non-flooded river terrace forests (Yáñez-Serrano et al., 2015).

2.2 Sampling design

We measured leaf and stem functional traits and VI E_c for 91 trees from 31 previously identified (with individual vouchers collected) and confirmed taxonomic woody species belonging to 16 families of angiosperms. Species were chosen from a preliminary selection based on their presence and abundance (in number of individuals per species) in the PELD-MAUA woody species inventory (Andreae et al., 2015) and available functional trait data for wood density and potential growth rate, obtained from local, regional, and global databases - Zanne et al. (2009); Reserva Adolpho Ducke Permanent Plots (PPBio, 2012); TRY Database (Kattge et al., 2011). Despite this preliminary selection, we measured functional traits *in situ* rather than relying on existing trait databases to obtain more realistic and comprehensive functional strategies for woody species prevalent in the Central Amazon Forest, many of which lacked data in current databases.

Species were distributed across four permanent plots along the ATTO access road (Supplementary Figure S1) covering: non-flooded upland (locally called *terra firme*, one plot); white sand (two plots); and ancient non-flooded river terrace (one plot) forests. These vegetation types are characterized by differences in soil and vegetation attributes. *Terra firme* vegetation is dense and mature, with a mean canopy height of 35 m (Gomes Alves et al., 2023), situated over highly weathered and well-drained ferralsols (Chauvel et al., 1987). White sand vegetation covers shrubby and forested

physiognomies, with canopies that reach from 12 to 20 m in height and various degrees of stratification (Demarchi et al., 2022). This vegetation sits on top of arenosols characterized by high water permeability, low water holding capacity, low specific heat capacity, and often a nutrient-poor organic layer (Quesada et al., 2011). River terrace soils are alisols, with a more recent pedogenetic status than *terra firme* ferralsols and a greater capacity to supply nutrients (Andreae et al., 2015).

We sampled species in plots of different vegetation types to maximize variation among species and allow capturing a broader range of CES. Since most species did not occur in all vegetation types, we could not repeat species across different vegetation types. In the case where a species would occur in more than one vegetation type, we sampled the species in the vegetation type where it was the most representative in terms of number of individuals and basal area. We sampled 2–5 trees for each species and selected trees that showed similar DBH values and represented maximum DBH values for their species at the plot (Table 1). Some species had fewer replicates than others due to technical issues in obtaining measurements of VI E_c and stomata-related traits for some individuals.

We measured VI E_c and leaf functional traits between November 20 - December 20, 2018 (early wet season); except for trees from *Mouriri duckeana*, *Pourouma minor*, *Protium hebetatum*, *Eschweilera coriacea*, and *E. grandiflora*, which were sampled between April 26 - May 5, 2019 (late wet season). Although isoprene emissions from Central Amazon Forest woody species vary seasonally as a function of leaf age (Alves et al., 2014, 2016; Gomes Alves et al., 2023), we assumed measurements were comparable since there was little variability in environmental variables between the two sampling periods (values of air temperature, relative humidity, photosynthetic active radiation, and precipitation relative to these periods are presented in the Supplementary Material; Supplementary Table S1), and forest canopies generally show similar fractions of mature leaves throughout the wet season (Lopes et al., 2016; Alves et al., 2018). Stem functional trait data was collected between October - December/2018, April - May/2019, and July/2019, since these traits show lower plasticity and seasonal variability.

2.3 Branch collection

A professional tree climber collected branches of at least 2 cm in diameter from the side of the tree crown that received direct light and hence did not contain shade-adapted leaves. Although we do not have precise information on leaf age, we avoided senescent and young leaves, as well as visibly unhealthy or damaged leaves and leaves with epiphylls. After being cut, branches were slowly lowered by rope and grabbed before touching the ground to prevent stomatal closure due to impact. Collected branches were identified, cut once again under water to prevent embolism formation in open vessels, and placed inside water bottles for transport to the field camp (where they were again cut under water to restore xylem flow before gas exchange and VI E_c

TABLE 1 Taxonomic species, family, vegetation type (*Terra firme*, dense non-flooded upland forest; White sand, white sand forest; River terrace, ancient non-flooded river terrace forest), range of diameter (minimum-maximum) at 1.3 m height (DBH; cm), and the number of trees measured per species for 31 Amazonian woody species evaluated in this study.

Species	Family	Vegetation type	DBH (min-max)	Trees/Species
Bocageopsis pleiosperma	Annonaceae	River terrace	16.2 - 28.7	3
Aspidosperma carapanauba	Apocynaceae	*Terra firme*	42.7 - 51.7	2
Geissospermum sericeum	Apocynaceae	*Terra firme*	17.2 - 51.0	3
Macoubea sprucei	Apocynaceae	White-sand	14.2 - 21.3	3
Protium grandifolium	Burseraceae	*Terra firme*	13.9 - 19.0	4
Protium hebetatum	Burseraceae	White sand	13.5 - 22.2	5
Pourouma minor	Cecropiaceae	River terrace	12.0 – 17.0	2
Croton matourensis	Euphorbiaceae	River terrace	17.3 - 22.0	3
Aldina heterophylla	Fabaceae	White sand	29.4 - 51.5	3
Inga alba	Fabaceae	River terrace	38.5 - 60.5	2
Macrolobium duckeanum	Fabaceae	White sand	10.4 - 12.8	3
Parkia igneiflora	Fabaceae	White sand	12.3 - 19.0	3
Swartzia reticulata	Fabaceae	*Terra firme*	37.4 - 38.8	2
Corythophora rimosa	Lecythidaceae	*Terra firme*	32.3 - 40.5	3
Eschweilera coriacea	Lecythidaceae	White sand	12.8 - 21.4	5
Eschweilera grandiflora	Lecythidaceae	*Terra firme*	11.0 - 39.3	5
Pachira faroensis	Malvaceae	White sand	12.7 - 17.2	3
Scleronema micranthum	Malvaceae	*Terra firme*	15.0 - 20.2	3
Theobroma sylvestre	Malvaceae	River terrace	10.1 - 12.0	3
Mouriri duckeana	Melastomataceae	River terrace	11.5 - 47.0	2
Trichilia schomburgkiana	Meliaceae	River terrace	16.0 - 17.3	2
Naucleopsis caloneura	Moraceae	*Terra firme*	14.5 - 17.0	3
Minquartia guianensis	Olacaceae	River terrace	34.5 - 41.0	3
Pagamea coriacea	Rubiaceae	White sand	14.0 - 16.1	3
Chrysophyllum sanguinolentum	Sapotaceae	White sand	22.0 - 35.7	3
Ecclinusa guianensis	Sapotaceae	*Terra firme*	14.5 - 29.7	2
Manilkara bidentata	Sapotaceae	White sand	14.5 - 20.2	3
Pouteria caimito	Sapotaceae	River terrace	11.1 - 16.2	3
Pradosia schomburgkiana	Sapotaceae	White sand	14.6 - 16.2	2
Simarouba amara	Simaroubaceae	River terrace	37.0 - 44.2	3
Rinorea guianensis	Violaceae	*Terra firme*	16.0 - 17.9	2

measurements). Due to the logistical issues involved in obtaining leaf-level physiological and VI measurements on intact branches from a large number of tall tropical trees (> 20 m height), performing measurements on cut branches in water is a broadly adopted, necessary practice to generate results capable of resolving ecological processes (Llusia et al., 2014; Albert et al., 2018; Jardine et al., 2020; Taylor et al., 2021; Gomes Alves et al., 2022, 2023; Robin

et al., 2024). Moreover, there is consistent evidence that cutting branches does not significantly compromise gas exchange or VI E_c measurements (Monson et al., 1994, 2016; Keller and Lerdau, 1999; Ghirardo et al., 2016). Finally, we selected one visibly mature and healthy leaf of the branch to measure VI E_c on-site, then we removed the branch from the water, wrapped the terminal piece in moist absorbent paper, and placed it in a closed plastic bag until

VI E_c measurements were finished (~ 15:00). Branches were processed in a field lab in the same day for functional trait measurements described below.

2.4 Leaf and stem functional trait measurements and calculations

We measured a total of 12 leaf traits: assimilation rate per dry mass (A_{mass}), stomatal conductance (g_s), foliar nitrogen per mass (N_{mass}), foliar phosphorus per mass (P_{mass}), leaf dry matter content (LDMC), leaf mass per area (LMA), leaf thickness (LT), force to tear (FtT), force to punch (FtP), vein density ($Vein_{Dens}$), stomatal density (St_{Dens}), stomatal guard cell length (St_{Lgth}); and four stem traits: wood density of stem (WD_{st}), wood density of twig (WD_{tw}), sapwood area per basal area (SABA) and total height per basal area (THBA). Leaf traits measured in this study are indicators of light capture and photosynthetic capacity (A_{mass}, g_s, N_{mass}, P_{mass}, LMA, St_{Dens}, and St_{Lgth}) and leaf defense and persistence (LDMC, LT, FtT, FtP, and $Vein_{Dens}$); while stem traits measured are related to biomechanical support, defense (WD_{st}, WD_{tw}, and THBA), and tolerance to drought (SABA) (Costa et al., 2018).

All functional trait measurements and calculations were performed according to published protocols (Pérez-Harguindeguy et al., 2013). We separated 3 leaves (including the leaf used to measure VI E_c) to measure leaf fresh and dry mass, leaf thickness (LT), and leaf area (LA). For the remaining leaf traits, we gathered a total of 8 leaves: 3 to measure force to punch (FtP), 3 to measure force to tear (FtT), and 2 for anatomical measurements (vein density, $Vein_{Dens}$; stomatal density, St_{Dens}; and stomatal guard cell length, St_{Lgth}). We weighed the leaves to obtain fresh mass and used a micrometer to measure LT and a table scanner to measure LA. Leaves were dried in an oven for 72 h at 60 °C and then weighed again to obtain dry mass. We measured FtP using a Pesola® scale (Medio spring scale, item n. 40300) modified with a pressure set (accessory for Medio-scales, item n. 4.004), and FtT using a tearing apparatus (Hendry and Grime, 1993). FtP and FtT were quantified in N mm^{-1}, considering that 1 kg of force is equivalent to 9.81 N; then FtP (N mm^{-1}) = ((FtP (g)/1000) * 9.81)/5.35 (mm) and FtT (N mm^{-1}) = FtT (kg) * 9.81/20 (mm) (Pérez-Harguindeguy et al., 2013). We analyzed images of scanned leaves with ImageJ software (Schneider et al., 2012) to obtain LA. We calculated specific leaf area (SLA) as the ratio of LA to leaf dry mass. We did not include petioles in the SLA calculation since they can be quite large for rainforest woody species and are usually more related to leaf positioning rather than biomass efficiency (Poorter et al., 2018). We calculated leaf dry matter content (LDMC) as the ratio of leaf dry mass to fresh mass, and leaf mass per area (LMA) as 1/SLA. Leaves used for LMA measurements were later ground using a portable blade mill, and their nutrient content was analyzed. Leaves set aside for anatomical measurements were cut in the median region, and the pieces were placed in plastic containers filled with FAA solution (Formaldehyde 37%, Glacial Acetic Acid, and Ethanol 70%) (Johansen, 1940) for 24 h, which was afterward replaced by Ethanol 70%. We processed stomatal density (St_{Dens}), stomatal guard cell length (St_{Lgth}), and vein density ($Vein_{Dens}$) at the Biodiversity and Functional Ecology Lab (National Institute for Amazonian Research - INPA) following established protocols (Johansen, 1940). Leaf nutrient content analysis was conducted by the Soil and Plant Thematic Lab (LTSP, INPA), following established protocols (EMBRAPA, 1999), and resulted in values of phosphorus (P_{mass}) and nitrogen (N_{mass}) per leaf dry mass. For compound leaves, we considered a leaflet as the laminar unit for all leaf measurements described above.

With an increment borer (diameter of 5.15 mm), we punctured the tree stem at 1.3 m height and penetrated the wood until the borer reached a depth of about half of the stem diameter (at 1.3 m height). Afterward, we extracted a core wood sample to measure fresh and dry mass, fresh volume, and active xylem depth. We cut and removed the bark of a 5 cm terminal piece of twig to measure the fresh and dry mass and fresh volume. We weighed twig and stem wood samples to obtain fresh mass, then measured fresh volume using the water displacement method. Wood samples were dried in an oven for 72 hrs at 105°C and weighed to obtain dry mass. We estimated the wood densities of twig (WD_{tw}) and stem (WD_{st}) as the ratio of wood dry mass to fresh volume. We estimated sapwood depth using a direct method of light transmission through the wood core sample (Cosme et al., 2017; Quiñonez-Piñón and Valeo, 2018). We placed the dried stem wood sample above a direct light source and, with a magnifying glass, observed and measured with a caliper the extension of open vessels throughout the length of the sample from cambium to pith. This method assumes that there is a higher concentration of tyloses in the heartwood than in the sapwood of angiosperm trees (Déjardin et al., 2010), making it possible to differentiate these parts of the xylem based on visual methods (Pfautsch et al., 2012). We obtained tree sapwood area (SA) by subtracting the heartwood area (area of extension of closed vessels) from the total basal area (BA), and then the ratio of sapwood area to basal area (SABA) was calculated. We measured the total height of the tree (TH) with the help of a tree climber, who placed a measuring tape on the highest point of the tree canopy and extended it until it reached the ground. With this value, we calculated the proportion of total height to the basal area (THBA).

2.5 Leaf volatile isoprenoid emission capacity analysis

We collected air samples for VI E_c measurements on-site using a LI-6400XT gas exchange portable system (LiCor, USA). We installed a hydrocarbon filter (Restek Pure Chromatography, Restek Corporations, USA) at the air inlet of the LI-6400XT to remove VIs from incoming ambient air. All tubing in contact with the sampling air was PTFE to avoid the release of VIs. Before each measurement, we obtained a chamber blank sample from the empty leaf chamber. We separately enclosed the leaf (for compound leaves we considered a leaflet as the laminar unit) in the leaf chamber under standard conditions (Photosynthetic photon flux density (PPFD) = 1000 μmol m^{-2} s^{-1}, leaf temperature = 30 °C) until net assimilation (A_n), stomatal conductance (g_s) and internal CO_2

concentration (C_i) were stable. The stability criterion for measurements was assigned up to one standard deviation of the mean A_n, and we visually monitored A_n until values reached a plateau, beginning measurements when the instrument had reached the plateau and the defined stability criterion. The flow rate of air going into the leaf chamber was 400 μmol s^{-1}, and CO_2 and H_2O concentrations were 400 μmol mol^{-1} and 21 mmol mol^{-1} (relative humidity of ~60%), respectively. An air sampling pump (GilAir$^{®}$ Plus, Levitt Safety, Canada), positioned downstream, routed air exiting the LI-6400XT leaf chamber to fill adsorbent cartridges (stainless steel tubes filled with Tenax TA and Carbograph 5 TD adsorbents) at a rate of 200 ml min^{-1} for 10 min, resulting in 2 L air samples for compound identification and quantification analyses in the lab. VIs accumulated in the adsorbent cartridges were determined by laboratory analysis at the Chemical Analysis Lab of the University of Amazonas State (UEA) immediately after each VI measurement campaign.

The cartridges were analyzed with a thermal desorption system (TD; Markes International, UK) interfaced with a gas chromatograph-mass spectrometer and flame ionization detectors (GC-MS-FID; 7890B-GC and 5977A-MSD series, Agilent Technologies, USA). We loaded the cartridges in the TD automatic sampler (TD-100, Markes International, UK), which connects to the thermal desorption system. Then, the collected samples were dried by purging for 5 min with 50 ml min^{-1} of ultrahigh-purity helium (all flow vented out of the split vent) before being transferred (300°C for 10 min with 50 sccm of ultrapure nitrogen) to the thermal desorption cold trap held at -10°C (Unity Series 1, Markes International, UK). During GC injection, the trap was heated to 300°C for 3 min while backflushing with a carrier gas (helium) at a flow rate of 6 ml min^{-1} directed into the column (HP-5, 5% phenyl methyl siloxane capillary, 30.0 m x 320 μm x 0.25 μm, Agilent Technologies, USA). The oven ramp temperature was programmed with an initial hold of 6 min at 27°C, followed by an increase to 85°C at 6°C min^{-1}, followed by a hold at 200°C for 6 min.

The GC-MS-FID was calibrated by injecting different amounts of gas standards into separate cartridges. The gas standard composition is shown in the Supplementary Material (Supplementary Table S2) (Apel & Riemer Environmental Inc., USA). The monoterpene composition of the cylinder reflected the most commonly observed monoterpenes emitted by Amazonian woody species (Jardine et al., 2015, 2017) which are also the most representative in terms of emissions at an ecosystem scale (Yáñez-Serrano et al., 2018). Calibration curves were carried out at least three times before the analysis of the sample cartridges, to get a mean correlation coefficient >= 0.98 (Supplementary Figure S2). In addition, two standard cartridges were analyzed every 20 samples to check system sensitivity. We identified isoprene and monoterpenes found in sample cartridges by comparison of observed retention times with the retention times of standards used for calibration. We identified and quantified compounds using Agilent Enhanced ChemStation (MSD ChemStation F.01.01.2317, Agilent Technologies, USA). We were not able to perform calibration

curves for α-Terpinene and p-Cymene, hence, α-Terpinene and p-Cymene found in our samples were calibrated with α-Pinene.

Concentration was determined using the sample volume that was passed through each cartridge. This volume is the integration of the mass flow rate measured and controlled by the pump used to suck the air coming out from the LI-6400XT leaf chamber. Once the volume mixing ratio of VI (ppbv) was obtained, VI emission capacity per area ($E_{c,A}$) was determined using the equation ($F = R$ppbv × Q/S), where F (nmol m^{-2} s^{-1}) is the leaf flux of VIs; Rppbv (nmol mol^{-1}) is VI concentration of the sample; Q is the flow rate of air into the leaf chamber (400 x 10^{-6} mol s^{-1}); S is the area of leaf within the chamber (0.0002 and 0.0006 m²). Values of $E_{c,A}$ for each monoterpene observed in samples were added to obtain the sum of monoterpene $E_{c,A}$ (from now on monoterpene E_c). Isoprene and monoterpene $E_{c,A}$ were transformed to emission capacity per dry mass (isoprene and monoterpene $E_{c,M}$) and A_n to photosynthesis per leaf dry mass (A_{mass}), all expressed in units of μg C g^{-1} h^{-1} to reflect carbon allocation dynamics in our analyses. We performed VI E_c measurements between 8:00 and 14:00 and measured trees from the same species in sequence, to reduce the effects of the plant's physiological circadian rhythm in the results. We did not see a significant variation between the time of measurements and A_n or g_s (Supplementary Figure S3), which suggests that a potential midday depression in stomatal conductance did not have a strong effect on our measurements.

2.6 Statistical analysis

We performed principal component analyses (PCA) with scaling to ordinate trees and species based on their functional trait values and to extract, from the multivariate space of trait correlations, the first two axes that captured most trait variation (PC1 and PC2). After that, we performed mixed effects linear regression models with species as a random factor to evaluate how PC1 and PC2 scores varied between vegetation types: PC1/PC2 ~ vegetation type + (1|Species). To evaluate if there were differences between PC1 and PC2 scores of trees from species with the capacity to emit isoprene or monoterpenes (0: non-emitter; 1: emitter), we performed mixed effects linear regression models with species as a random factor: PC1/PC2 ~ capacity to emit isoprene/monoterpenes + (1|Species).

Given that the capacity to emit isoprene or monoterpenes could be limited by both ends of the fast-slow spectrum (H1), we tested whether emitters were significantly positioned (lower variance) on the PC axes than non-emitters by producing bootstrapped distributions of variance differences (non-emitter variance minus emitter variance) based on iterative random sampling of PC values from each group (emitter/non-emitter) with replacement. To test whether PC1 and PC2 scores of trees from species with the capacity to emit isoprene or monoterpenes (0: non-emitter; 1: emitter) varied between vegetation types, we performed mixed effects linear regression models with species as a random factor: PC1/PC2 scores of isoprene/monoterpene emitters ~ vegetation type +

(1|Species); and PC1/PC2 scores of isoprene/monoterpene non-emitters ~ vegetation type + (1|Species).

To compare magnitudes of isoprene and monoterpene E_c between vegetation types, we performed mixed effects linear regression models with species as a random factor: isoprene $E_{c,M}$/ monoterpene $E_{c,M}$ ~ vegetation type + (1|Species). To evaluate which variables (PC1, PC2, or vegetation type) best explained variations in the magnitudes of isoprene and monoterpene E_c, we performed a stepwise model selection analysis. Statistical analyses of the magnitudes of isoprene and monoterpene E_c were always performed with log-transformed + 1 values of isoprene and monoterpene $E_{c,M}$, and only included individual trees from species with the capacity to emit isoprene and/or monoterpenes.

To test if there was a tradeoff in the capacity to emit isoprene or monoterpenes, we performed a chi-squared (χ^2) analysis to compare observed and expected occurrences of species that only emitted isoprene, only emitted monoterpenes, emitted both isoprene and monoterpenes, or did not emit either isoprene or monoterpenes. Lastly, we performed a mixed effects linear regression model with species as a random factor to test if there was a tradeoff in the magnitudes of isoprene and monoterpene E_c in trees from species with the capacity to emit both compounds: isoprene $E_{c,M}$ ~ monoterpene $E_{c,M}$ + (1|Species).

Because isoprene and monoterpene synthase encoding genes should be conserved at the taxonomic species level (Dani et al., 2014; Loreto and Fineschi, 2015), trees that did not show detectable E_c but belonged to species with the capacity to emit isoprene/ monoterpenes were assigned as 1/"Yes" in mixed effects models comparing emitters and non-emitters. Similarly, we included 0 values from trees that did not show detectable E_c but belonged to species with the capacity to emit isoprene/monoterpenes in mixed effects models comparing magnitudes of isoprene and monoterpene E_c. We chose this statistical approach because an absence of detectable E_c in plants from emitting species can be attributed to high intraspecific variability in enzyme activities and precursor concentrations at the MEP pathway, which has been shown to lead to differences up to seven times between different plants of the same species even when grown under the same conditions (Lehning et al., 1999; Owen and Peñuelas, 2013; Zeng et al., 2024).

Mixed effects linear regression models were performed using the lmer function of the LME4 R package (Bates et al., 2015), and results are presented as plots from the GGPLOT2 package (Wickham, 2016). The p-values of pairwise comparisons between vegetation types and linear regressions were obtained with the EMMEANS package (Lenth, 2024). All statistical analyses were performed using R version 4.3.2 through the platform RStudio 2023.9.1.494 (R core team, 2023).

3 Results

We observed the capacity to emit isoprene in 39 trees from 14 species (45% of species) and to emit monoterpenes in 49 trees from 27 species (87% of species) (Table 2, Figure 1). The most frequent

emitted monoterpenes were α-terpinene (34 trees), followed by β-pinene (16 trees) and β-phellandrene (12 trees), but we also saw trees emitting camphene (3 trees), α-pinene (2 trees), p-cymene (2 trees), and β-myrcene (1 tree) (Supplementary Table S3). The average intra-specific variation in the magnitudes of VI E_c was lower than the inter-specific variation (Table 2). Magnitudes of isoprene E_c varied from 2.1 - 54.3 μgC g^{-1} h^{-1}, with one tree from *Swartzia reticulata* emitting 150 μgC g^{-1} h^{-1}, and of monoterpene E_c varied from 0.2 - 32.1 μgC g^{-1} h^{-1}. Complete names, units, standard deviation, range in dataset, and average percentages of intra- and inter-specific variation in VI E_c and functional traits are presented in Table 2. Average values per species and percentages of intra-specific variation are available in the Supplementary Material (Appendix 1). Species that emitted and did not emit isoprene were similarly distributed between different vegetation types, but *terra firme* did not contain non-emitters of monoterpenes (Figure 1). Chi-squared (χ^2) analysis of observed and expected occurrences of species that only emitted isoprene, only emitted monoterpenes, emitted both isoprene and monoterpenes, or did not emit either isoprene or monoterpenes was not statistically significant (Table 3).

The PCA performed with all trees revealed trait correlations that formed two main, partially independent principal component axes (PC1-2) of CES (Figure 2A) and, together, explained 43.2% of the variance in functional trait data. The PCA performed with species average functional trait values reflected similar correlations as the PCA performed with all trees and showed only a slightly higher percentage of variation explained by PC1 and PC2 (46.9%; Supplementary Figure S4). Functional traits > 20% correlated with PC1 and/or PC2 and percentages (%) of correlation are presented in Figure 2B. Loadings for all PC axes and scores are presented in the Supplementary Material (Appendix 1).

PC1 axis showed functional trait correlations that reflected fast-slow leaf CES. Trees with more negative scores for this axis had higher N_{mass} and P_{mass}, were thinner and wider (low LT and LMA), had higher densities of smaller stomata (high St_{Dens} and low St_{Lght}), and weaker mechanical resistance (low FtP); thus being considered to have faster leaf strategies. Meanwhile, trees with more positive PC1 scores had lower N_{mass} and P_{mass}, were thicker, narrower, and tougher (high LT, LMA, and FtP), and had lower densities of larger stomata (low St_{Dens} and high St_{Lght}); thus being considered to have slower leaf strategies.

PC2 axis captured a mix of leaf (A_{mass}, g_s, FtP, St_{Dens}) and stem (WD_{st}, WD_{tw}, and SABA) CES. Trees with more negative scores for this axis were trees with higher A_{mass} and g_s, lower stomatal density (St_{Dens}), weaker leaves (low FtP), and higher proportional area of active xylem vessels (SABA) and less dense wood (low WD_{st} and WD_{tw}); hence being considered to have faster leaf/stem CES. Meanwhile, trees with more positive PC2 scores had lower A_{mass} and g_s, higher stomatal density (St_{Dens}), tougher leaves (high FtP), and lower proportional area of active xylem vessels (SABA) and denser woods (high WD_{st} and WD_{tw}); hence being considered to have slower leaf/stem CES. Pairwise comparisons did not show significant differences in PC1 values between vegetation types (Figure 3A) but revealed that trees from *terra firme* showed
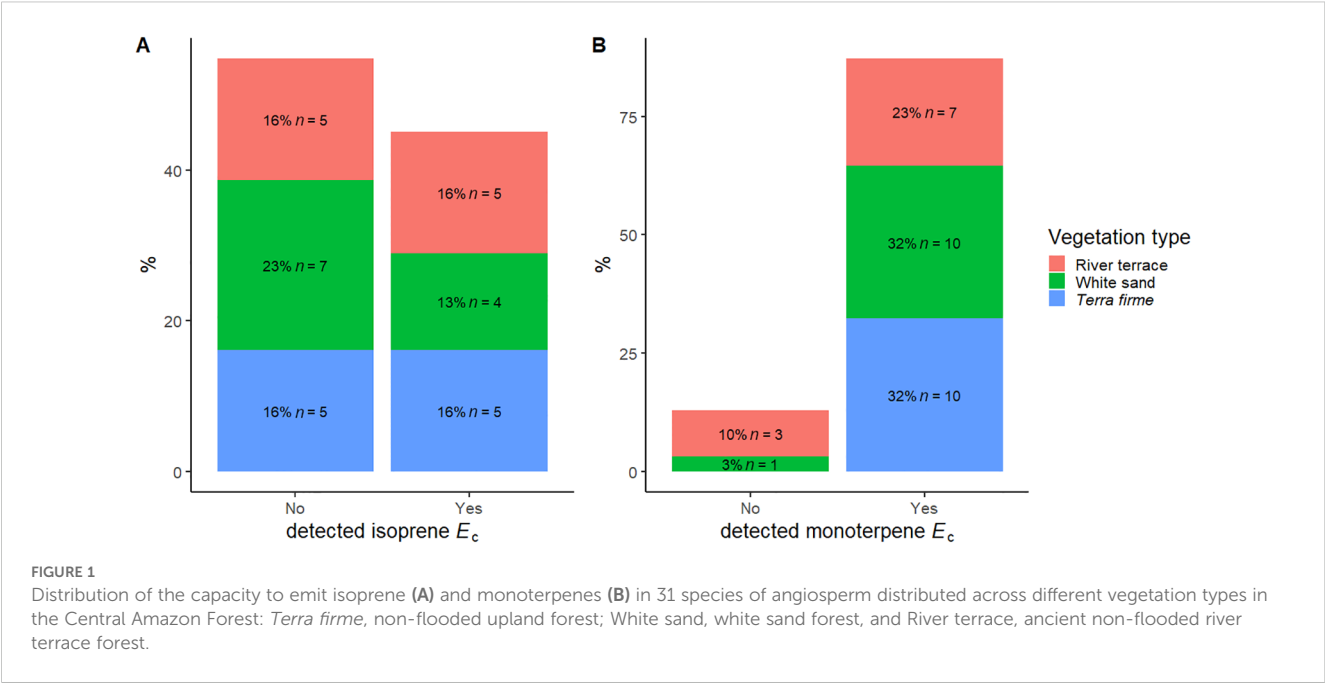
TABLE 2 Complete names, units, values of mean, standard deviation (SD), range in dataset, average (avg) intra-specific variation, and inter-specific variation of magnitudes of isoprene and monoterpene $E_{c,A}$ and $E_{c,M}$, and functional traits measured for 91 trees from 31 species of angiosperm in a Central Amazon Forest.

Variable	Unit	Mean	SD	Range in dataset	avg intra-specific variation %	inter-specific variation %
Isoprene emission capacity per area (Isoprene $E_{c,A}$)	nmol m^{-2} s^{-1}	4.7	9.9	0 - 81.6	68.6	178.0
Isoprene emission capacity per dry mass (Isoprene $E_{c,M}$)	µgC g^{-1} h^{-1}	8.8	18.8	0 - 150.9	70.4	182.3
Sum of monoterpene emission capacity per area (Monoterpene $E_{c,A}$)	nmol m^{-2} s^{-1}	0.6	1.3	0 - 7.3	104.1	118.0
Sum of monoterpene emission capacity per dry mass (Monoterpene $E_{c,M}$)	µgC g^{-1} h^{-1}	2.6	5.4	0 - 32.1	104.9	124.0
Net assimilation rate (A_n)	µmol m^{-2} s^{-1}	5.8	3.4	0.13 - 20.6	31.8	55.4
Assimilation rate per dry mass (A_{mass})	µgC g^{-1} h^{-1}	2 130.6	1 377.7	51.2 - 8998.5	30.2	63.3
Stomatal conductance (g_s)	mol m^{-2} s^{-1}	0.1	0.07	0.01 - 0.3	38.3	51.0
Foliar nitrogen per mass (N_{mass})	mg g^{-1}	16.2	5.3	7.55 - 32.9	8.4	32.9
Foliar phosphorus per mass (P_{mass})	mg g^{-1}	0.7	0.2	0.39 - 1.4	11.9	26.6
Leaf dry matter content (LDMC)	mg g^{-1}	464.0	66.5	318.3 - 650.4	7.8	12.6
Specific leaf area (SLA)	cm^2 g^{-1}	88.0	29.3	42.6 - 197.2	12.2	30.7
Leaf mass per area (LMA)	g cm^{-2}	0.01	0.004	0.005 - 0.02	12.2	30.7
Leaf thickness (LT)	mm	0.3	0.09	0.2 - 0.6	9.4	32.6
Force to Tear (FtT)	N mm^{-1}	1.0	0.6	0.2 - 2.9	18.8	62.0
Force to Punch (FtP)	N mm^{-1}	0.2	0.1	0.05 - 0.5	18.2	38.8
Vein density ($Vein_{Dens}$)	veins mm^{-2}	8.6	2.3	1.8 - 15.0	13.9	24.6
Stomatal density (St_{Dens})	stomata mm^{-2}	0.3	0.2	0.02 - 0.8	21.6	57.0
Stomatal guard cell length (St_{Lgth})	µm	12.9	9.0	5.7 - 45.3	20.2	66.2
Wood density of stem (WD_{st})	g cm^{-3}	0.7	0.2	0.29 - 0.93	8.7	22.7
Wood density of twig (WD_{tw})	g cm^{-3}	0.7	0.1	0.39 - 0.85	6.4	14.3
Sapwood area per basal area (SABA)	m^2 m^{-2}	0.7	0.3	0.08 - 1	14.9	36.7
Total height per basal area (THBA)	m m^{-2}	657.7	417.4	57.8 - 1899.0	33.8	56.1

Percentage (%) of average intra-specific variation was calculated by averaging the observed coefficients of variation > 0 (CV, CV = (SD/mean) * 100) for each variable within each species, and of inter-specific variation was calculated as the CV of average values per species for each variable. Mean values per species and intra-specific variation are provided in the Supplementary Material (Appendix 1).

significantly slower leaf/stem CES strategies (more positive PC2 scores) compared to trees from river terrace (Figure 3B).

We did not observe significant differences in mean values of PC1/PC2 between emitters and non-emitters of isoprene or monoterpenes (Figure 4). However, bootstrapped analyses comparing PC score variances between emitters and non-emitters showed that isoprene emitters tended to be positioned (lower PC2 variance, inset Figure 4B) at the slower end of leaf/stem CES (positive PC2 scores) compared to non-emitters of isoprene (Figure 4B). This analysis also revealed that monoterpene emitters occupied the entire range of PC1 and PC2 values and that non-emitters of monoterpenes were rare and significantly positioned (lower variance, insets Figures 4C, D) at the faster end of leaf CES

(negative PC1 scores) and the slower end of fast/stem CES (positive PC2 scores) (Figures 4C, D).

Pairwise comparisons of PC1/PC2 scores between different vegetation types (Supplementary Figure S5) showed that non-emitters of isoprene from white sand had significantly slower leaf CES (more positive PC1) than respective non-emitters from the river terrace (Supplementary Figure S5A). It also showed that monoterpene emitters from *terra firme* had significantly slower leaf and stem CES (more positive PC2) than respective emitters from the river terrace (Supplementary Figure S5D). These are patterns that reflect the already observed distribution of CES across vegetation types (Figure 2), and there were no significant differences in magnitudes of isoprene and monoterpene E_c between vegetation types (Figure 5).

FIGURE 1
Distribution of the capacity to emit isoprene **(A)** and monoterpenes **(B)** in 31 species of angiosperm distributed across different vegetation types in the Central Amazon Forest: *Terra firme*, non-flooded upland forest; White sand, white sand forest, and River terrace, ancient non-flooded river terrace forest.

The stepwise model selection analysis (Table 4) revealed that PC2 and PC1 were consistently significant predictors of the magnitudes of isoprene and monoterpene E_c, respectively. This analysis also confirmed that vegetation type did not have a strong effect on variation in magnitudes of isoprene and monoterpene E_c, given that the models containing only PC2 for isoprene E_c and only PC1 for monoterpene E_c had the lowest Akaike Information Criterion (AIC) (Table 4). Mixed effects linear regression models between magnitudes of isoprene/monoterpene E_c and PC1/PC2 (Figure 6) showed that isoprene E_c significantly increased toward slower leaf and stem CES (Figure 6B, more positive PC2 scores) while monoterpene E_c significantly increased toward faster leaf CES (Figure 6C, more negative PC1 scores). Finally, there was no significant relationship between the magnitudes of isoprene and monoterpene E_c in trees from species with the capacity to emit both compounds (Supplementary Figure S6).

4 Discussion

To understand how volatile isoprenoid (VI) emissions varied with plant carbon economics strategies (CES) we present here what is, to our knowledge, the most comprehensive suite of isoprene and monoterpene emission capacity (E_c) measurements, in tandem with leaf and stem functional trait data for 91 trees from 31 species of angiosperm 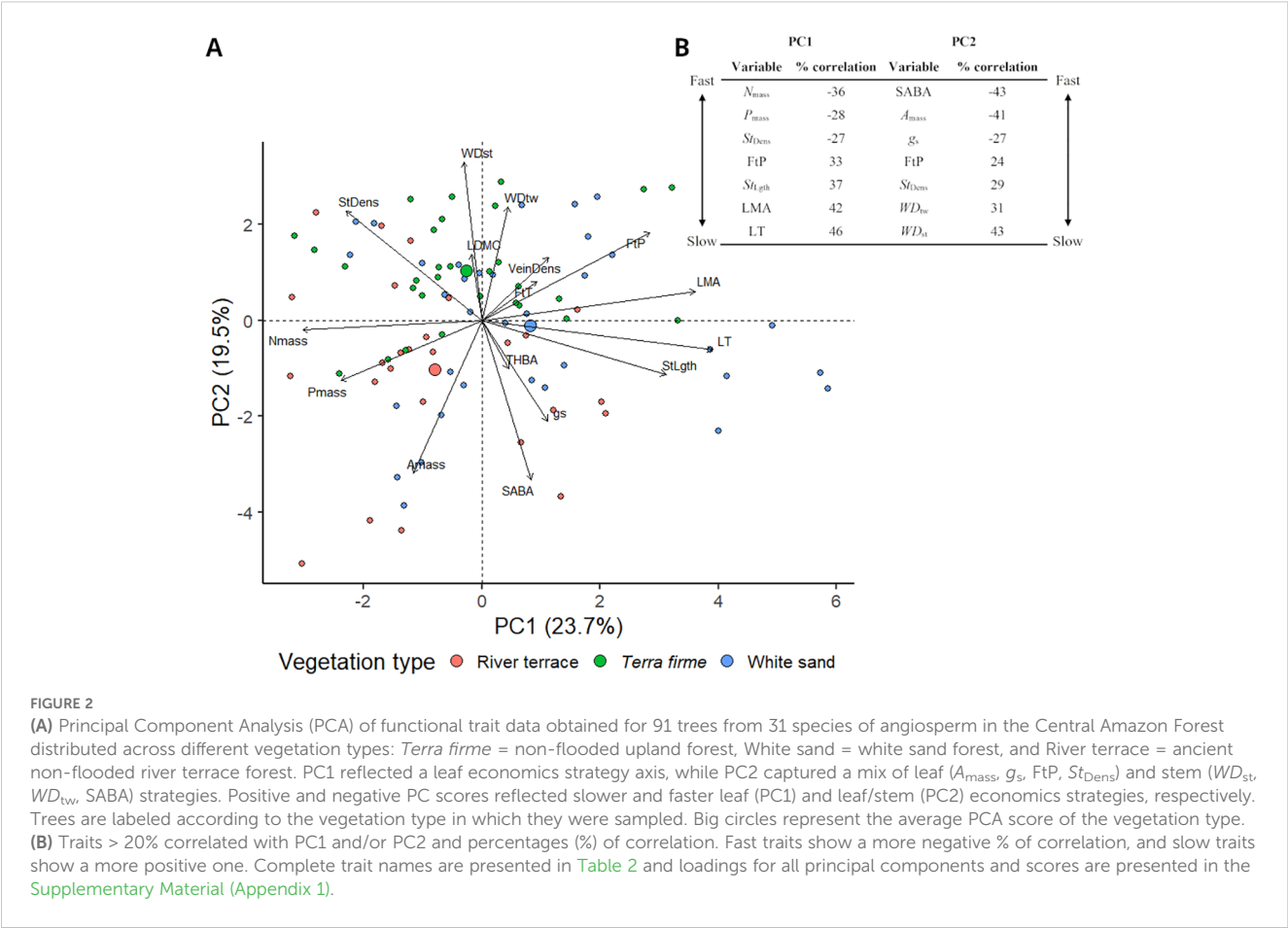occurring in different vegetation types (non-flooded upland *terra firme*, white sands, and ancient non-flooded river terrace forests) in the Central Amazon Forest, with many of these measurements representing the first-ever recorded data for numerous woody species. The capacity to emit monoterpenes was observed in 27 out of 31 species, and monoterpene emitters occupied the whole range of CES captured in our PCA, but magnitudes of monoterpene E_c increased toward faster leaf strategies. Meanwhile, the capacity to emit isoprene was observed in 14 species; isoprene emitters tended to be positioned toward slower leaf/stem CES, and magnitudes of isoprene E_c also increased toward slower leaf and stem CES. Finally, despite potential carbon economic limitations, the capacity to emit isoprene or monoterpenes showed no evidence of mutual exclusion, and magnitudes of isoprene and monoterpene E_c from trees of species with the capacity to emit both compounds did not vary simultaneously.

4.1 Principal component analysis of leaf and stem functional traits

We performed a principal component analysis (PCA) with traits measured *in situ* instead of relying on existing databases to obtain more realistic and comprehensive functional strategies for woody species prevalent in the Central Amazon Forest, many of which lacked data in current databases. Despite reflecting a smaller range of strategies than larger-scale studies (Wright et al., 2004;

TABLE 3   Contingency table and chi-squared (χ^2) p-value of comparison between observed and expected occurrences of the capacity to emit isoprene and monoterpenes in 31 species of angiosperm in a Central Amazon Forest.

	No monoterpene E_c	Monoterpene E_c	χ^2 p-value
No isoprene E_c	2	15	1.0
Isoprene E_c	2	12	

FIGURE 2
(A) Principal Component Analysis (PCA) of functional trait data obtained for 91 trees from 31 species of angiosperm in the Central Amazon Forest distributed across different vegetation types: *Terra firme* = non-flooded upland forest, White sand = white sand forest, and River terrace = ancient non-flooded river terrace forest. PC1 reflected a leaf economics strategy axis, while PC2 captured a mix of leaf (A_{mass}, g_s, FtP, St_{Dens}) and stem (WD_{st}, WD_{tw}, SABA) strategies. Positive and negative PC scores reflected slower and faster leaf (PC1) and leaf/stem (PC2) economics strategies, respectively. Trees are labeled according to the vegetation type in which they were sampled. Big circles represent the average PCA score of the vegetation type. **(B)** Traits > 20% correlated with PC1 and/or PC2 and percentages (%) of correlation. Fast traits show a more negative % of correlation, and slow traits show a more positive one. Complete trait names are presented in Table 2 and loadings for all principal components and scores are presented in the Supplementary Material (Appendix 1).

Kattge et al., 2011; Pérez-Harguindeguy et al., 2013; Díaz et al., 2016; Segrestin et al., 2021), our functional trait dataset contained ranges of trait values similar to those observed in other tropical studies (Baraloto et al., 2010b, 2010a; Costa et al., 2018; Vleminckx

et al., 2021). We measured functional traits from species across different vegetation types to capture a broader range of CES, and trees from *terra firme* showed significantly slower leaf/stem CES compared to river terrace trees (Figure 2). This result could be
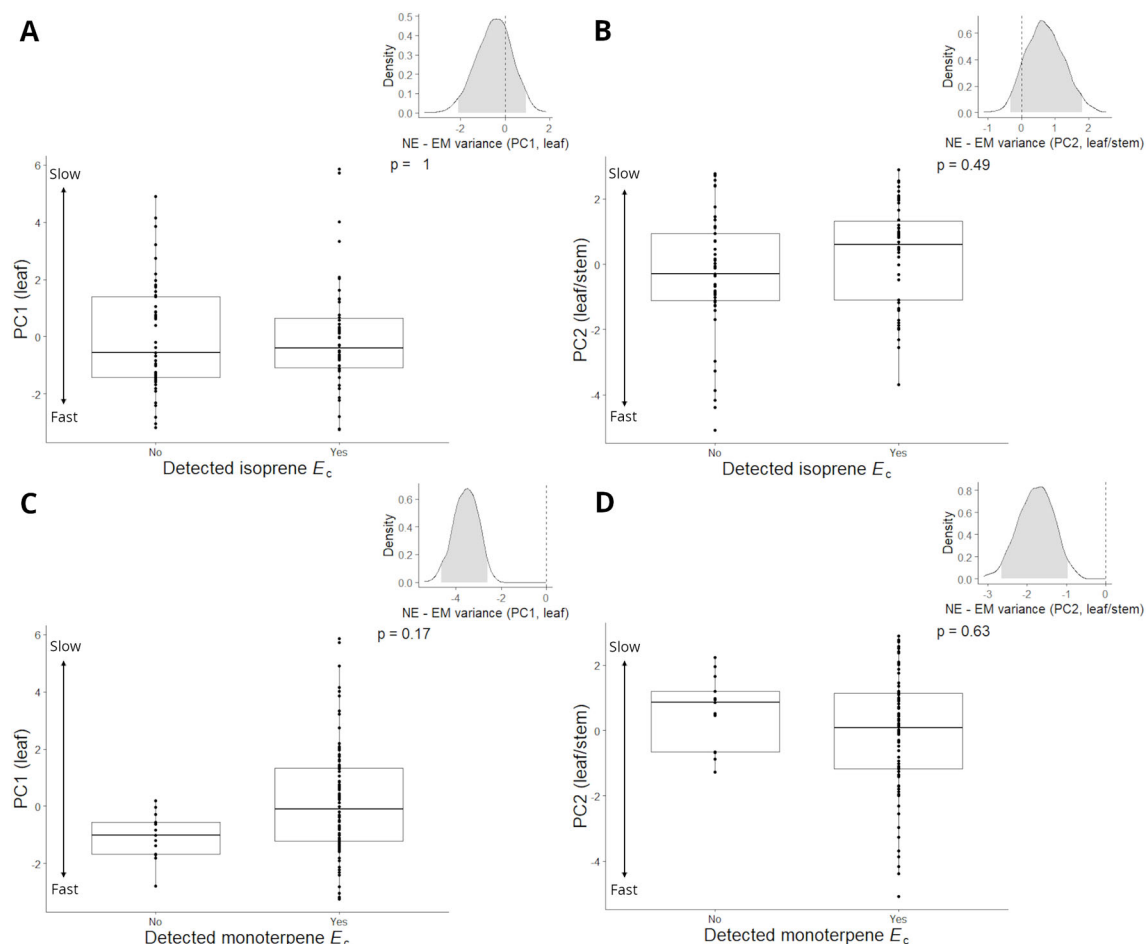

FIGURE 3
Pairwise comparisons of PC1 **(A)** and PC2 **(B)** scores between pairs of vegetation types for 91 trees from 31 species of angiosperm in the Central Amazon Forest distributed across different vegetation types: *Terra firme*; non-flooded upland forest, White sand; white sand forest, and River terrace; ancient non-flooded river terrace forest. Negative and positive PC scores reflected faster and slower leaf (PC1) and leaf/stem (PC2) economics strategies, respectively. Pairwise comparisons are mixed effects models that were performed with all trees (n = 91) and included species as a random factor.

FIGURE 4
Pairwise comparisons of isoprene emitter and non-emitter (Detected isoprene E_c; Yes, No) PC1 **(A)** and PC2 **(B)** scores, and monoterpene emitter and non-emitter (Detected monoterpene E_c; Yes, No) PC1 **(C)** and PC2 **(D)** scores for 91 trees from 31 species of angiosperm in the Central Amazon Forest. Negative and positive PC scores reflected faster and slower leaf (PC1) and leaf/stem (PC2) economics strategies, respectively. Pairwise comparisons are mixed effects models that were performed with all trees (n = 91) and included species as a random factor. Inset graphs show density distributions of bootstrapped resampled variances of average PC1/PC2 non-emitter (NE variance) minus emitter (EM variance) scores for isoprene/monoterpenes. Density distribution analyses were performed with species averages (n = 31) of PC1 and PC2 scores.

explained by the fact that not only river terrace soils provide greater nutrient supply than *terra firme* soils, but the latter is also situated much more distant from the water table (Andreae et al., 2015) and is likely more vulnerable to drought (Costa et al., 2023) compared to the first. These are factors that possibly influenced leaf and stem traits from *terra firme* toward slower CES compared to river terrace, but more research would be needed to confirm this.

Furthermore, trees from the white sand forest had marginally significant (p = 0.09) slower leaf traits compared to trees from the river terrace, and this relationship was more evident (p = 0.04) in isoprene non-emitters. The sandy and generally nutrient-poor arenosols from white sand forests (Quesada et al., 2011) probably influenced leaf traits in this vegetation toward more resource-conservative, slow strategies (Demarchi et al., 2022). Still, this relationship was only significant for isoprene non-emitters, and this could be because, despite possible environmental drivers, river terrace trees with the capacity to emit isoprene had their trait compositions more directed toward slower leaf CES - as isoprene

emitters tended to be positioned toward slower leaf/stem CES regardless of vegetation type - but the effect was not statistically significant (p = 0.26, Supplementary Figure S7).

Meanwhile, our analysis retrieved classic relationships from the leaf economics spectrum (Wright et al., 2004), such as positive correlations between N_{mass} and P_{mass}, with both being negatively correlated with LMA. It also retrieved relationships from previously proposed wood and whole-plant economics spectrum (Chave et al., 2009; Reich, 2014), with positive correlations between A_{mass} and g_s, both negatively correlated with wood density (WD_{st}, WD_{tw}). Although we measured traits in leaves from collected branches that were receiving full direct sunlight at least during part of the day and did not contain shade-adapted leaves, we understand that, given the constant fluctuations in canopy openness observed in tropical forests (Chazdon and Fetcher, 1984; Valladares et al., 2000; Montgomery and Chazdon, 2001), these leaves possibly did not develop under high light conditions as predicted by the leaf economics spectrum (Wright et al., 2004). Since this could have
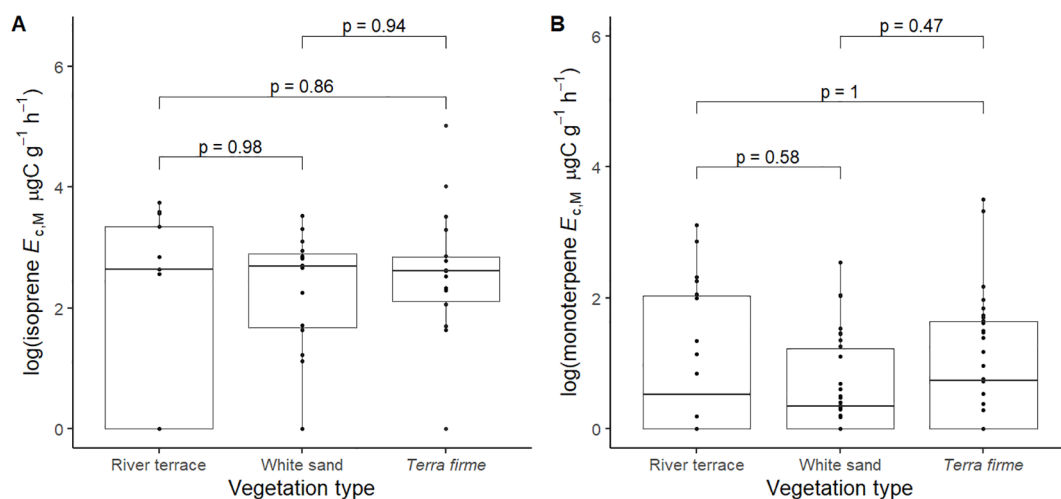
FIGURE 5
Pairwise comparisons of log + 1 of isoprene emission capacity per leaf dry mass (isoprene $E_{c,M}$, µg C g^{-1} h^{-1}) **(A)** and log + 1 of monoterpene emission capacity per leaf dry mass (monoterpene $E_{c,M}$, µg C g^{-1} h^{-1}) **(B)** between pairs of vegetation types: *Terra firme* = non-flooded upland forest, White sand = white sand forest, and River terrace = ancient non-flooded river terrace forest. Pairwise comparisons are mixed effects models that were performed with all trees from species that showed capacity to emit isoprene (**A**, *n* = 46) and monoterpenes (**B**, *n* = 78) and included species as a random factor.

influenced leaf traits that are more affected by light-driven trait plasticity, we tried to overcome this issue by performing a PCA with mass-based traits (LMA, A_{mass}, N_{mass}, and P_{mass}), which are less affected by shading during leaf development (Legner et al., 2014; Keenan and Niinemets, 2016; Martin et al., 2020).

Parallel to this, St_{Dens} was strongly - yet opposite - correlated with both PCs. In PC1, it is possible that the negative correlation between St_{Dens} (N_{mass} and P_{mass}) and St_{Lgth} (LMA and FtP) reflects a type of tradeoff where leaves with faster CES could be able to maximize CO$_2$ assimilation while minimizing water loss - by having higher N_{mass}, P_{mass}, and a higher density of smaller stomata (Hetherington and Woodward, 2003; Sack and Buckley, 2016). Log-scale pairwise standard major axis (SMA) regressions among these traits corroborated the directions of these relationships but showed that they sometimes differed in statistical significance between isoprene emitters and non-emitters (Supplementary Figure S8). For instance, only isoprene emitters showed significant relationships between St_{Dens}, N_{mass}, LMA, and FtP, and between St_{Lgth}, N_{mass}, LMA, and FtP.

At the same time, the negative correlations between St_{Dens} (WD_{st} and FtP) and g_s (A_{mass} and SABA) in PC2 perhaps reflected more multiple and integrated leaf/stem CES strategies. In this axis, trees with faster CES perhaps have their higher growth demands met by increased A_{mass}, g_s, and SABA, while controlling for water loss with a decreased density of stomata. Meanwhile, trees with slower CES possibly balance carbon assimilation and mechanical/hydraulic resistance by increasing St_{Dens} while decreasing SABA and increasing WD_{st} - since narrower active xylem vessels with thicker walls (i.e., more fiber) relative to lumen area are less likely to collapse under drought (Hacke et al., 2001; Poorter et al., 2010; Hoffmann et al., 2011; Cosme et al., 2017). Log-scale pairwise SMA regressions showed that these traits followed these relationships only for isoprene emitters and were actually opposite for non-emitters, although statistical significance in these relationships for

isoprene emitters was not achieved (Supplementary Figure S9). The integrated leaf/stem relationships observed in this second axis also corroborate the view from Reich (2014); however, trees and species were not completely aligned when comparing the first and second axes, which also corroborates the view from Baraloto et al. (2010a) that leaf and stem strategies may be decoupled in tropical forest woody species.

4.2 Volatile isoprenoid emissions and carbon economics strategies

Considering the idea of a balance between the benefits of VI production for plant defense and survival and the associated carbon costs of VI production, we hypothesized that (H1) the capacity to emit and magnitude of isoprene or monoterpene E_c varied with CES, and were either (H1a) associated with faster CES due to higher photosynthetic requirements to cover carbon demands of emissions, or (H1b) associated with slower strategies where higher carbon demands were compensated by greater tissue longevity. We observed the capacity to emit monoterpenes in trees distributed throughout the entire range of CES retrieved in our PCA, but the magnitudes of monoterpene E_c increased toward faster leaf strategies (supporting H1a). Meanwhile, trees with the capacity to emit isoprene were concentrated toward slower leaf/ stem CES, and magnitudes of isoprene E_c also increased toward slower leaves and stems (supporting H1b). Finally, the distribution of leaf and stem strategies between vegetation types was generally consistent within emitters and non-emitters of isoprene and monoterpenes, and vegetation type was not a strong or significant predictor of variation in emission rates.

Both isoprene and light-dependent monoterpenes are produced in the methyl-erythritol 4-phosphate (MEP) pathway from recently assimilated photosynthetic carbon and serve roles in abiotic stress

TABLE 4 Stepwise model selection analysis table showing Akaike Information Criterion (AIC) and significant predictors (Sig.) of different models with increased complexity.

Independent variable (y)	Model	AIC	Sig.
log(Isoprene $E_{c,M}$ + 1)	y ~ 1 + (1|Species)	142.1	
	y ~ PC1 + (1|Species)	145.1	
	y ~ PC2 + (1|Species)	**141.2**	*** PC2**
	y ~ Vegetation + (1|Species)	143.8	
	y ~ PC1 + PC2 + (1|Species)	145.3	* PC2
	y ~ PC1 + Vegetation + (1|Species)	146.9	
	y ~ PC2 + Vegetation + (1|Species)	142.6	* PC2
	y ~ PC1 + PC2 + Vegetation + (1|Species)	146.6	* PC2
log(Monoterpene $E_{c,M}$ + 1)	y ~ 1 + (1|Species)	216.3	
	y ~ PC1 + (1|Species)	**214.6**	**** PC1**
	y ~ PC2 + (1|Species)	221.2	
	y ~ Vegetation + (1|Species)	219.6	
	y ~ PC1 + PC2 + (1|Species)	219.8	* PC1
	y ~ PC1 + Vegetation + (1|Species)	219.4	* PC1
	y ~ PC2 + Vegetation + (1|Species)	223.7	
	y ~ PC1 + PC2 + Vegetation + (1|Species)	223.8	* PC1

(*) p < 0.05 and (**) p < 0.01. Models with lowest AIC are in bold.

protection (Loreto et al., 1996; Jardine et al., 2015, 2017; Sharkey and Monson, 2017; Monson et al., 2021; Srikanth et al., 2024). Compared to isoprene, monoterpenes contain double the amount of carbon atoms in their molecules, present more complex chemical structures (e.g., acyclic, monocyclic, bicyclic) (Thulasiram et al., 2007), and are produced one chemical reaction step later (Zhao et al., 2013). However, the seemingly elevated construction costs of monoterpenes compared to isoprene might be outweighed by the fact that these compounds have additional wider ecological functions (e.g., herbivore deterrence, plant signaling), provide specialist support at different temperatures (Jardine et al., 2017; Byron et al., 2022), and are preferably produced over isoprene due to stronger enzyme affinities in the preceding steps of the MEP pathway (Harrison et al., 2013).

Even though isoprene has also been reported to influence herbivore decision (Frank et al., 2021; Pollastri et al., 2021), the extensive structural variability of monoterpene compounds may provide a significant advantage in deterring generalist herbivores and promoting the coexistence of plant species by enhancing overall chemical diversity (Salazar et al., 2018; Vleminckx et al., 2018). Therefore, monoterpene emissions should be particularly advantageous in such an ecologically complex and species-diverse tropical forest like the Amazon Forest (Asner et al., 2014; Sakschewski et al., 2016; Cardoso et al., 2017; Massad et al., 2017), which perhaps explains why the capacity to emit monoterpenes was observed in trees distributed throughout the whole range of CES (Joo et al., 2018) captured in our PCA.

Meanwhile, trees with the capacity to emit isoprene showed a tendency to be concentrated toward slower leaf and stem CES, and

the magnitude of isoprene E_c also increased toward slower leaves and stems. Isoprene had been previously associated with faster leaf economics strategies due to observed relationships between higher isoprene emission rates, higher photosynthetic capacity, and shorter leaf lifespan (Harrison et al., 2013; Dani et al., 2014), in addition to its possible role as a thermoprotector and hypothesized sink of excess energy (Singsaas et al., 1997; Behnke et al., 2007; Morfopoulos et al., 2013; Pollastri et al., 2014, 2019). However, isoprene is currently viewed under a more holistic perspective, being suggested to be a metabolite that coordinates gene expression and mediates resource supply and demand in stress responses (Monson et al., 2021).

In this context, studies have recently observed relationships between the capacity to emit and the magnitude of isoprene E_c and increased accumulation of lignin and leaf toughness (Fernández-Martínez et al., 2018; Zuo et al., 2019; Monson et al., 2020, 2021; Yuan et al., 2020; Robin et al., 2024). Leaf toughness (Force to Punch, FtP) was a trait contained within the PC2 axis, suggesting that the association between isoprene emissions and increased leaf mechanical resistance may extend itself to increased stem resistance, but more research would be needed to test this hypothesis. Nevertheless, the observed association between the presence and magnitude of isoprene emission capacity and slower CES may reflect an underlying trade-off between investment in growth- and defense-related traits. More specifically, isoprene emitters perhaps prioritize structural defenses (e.g., increased leaf toughness and stem resistance) over traits linked to rapid resource acquisition (e.g., high N_{mass} and P_{mass}). Such a trade-off is consistent with recent perspectives on the multifunctional role of isoprene,
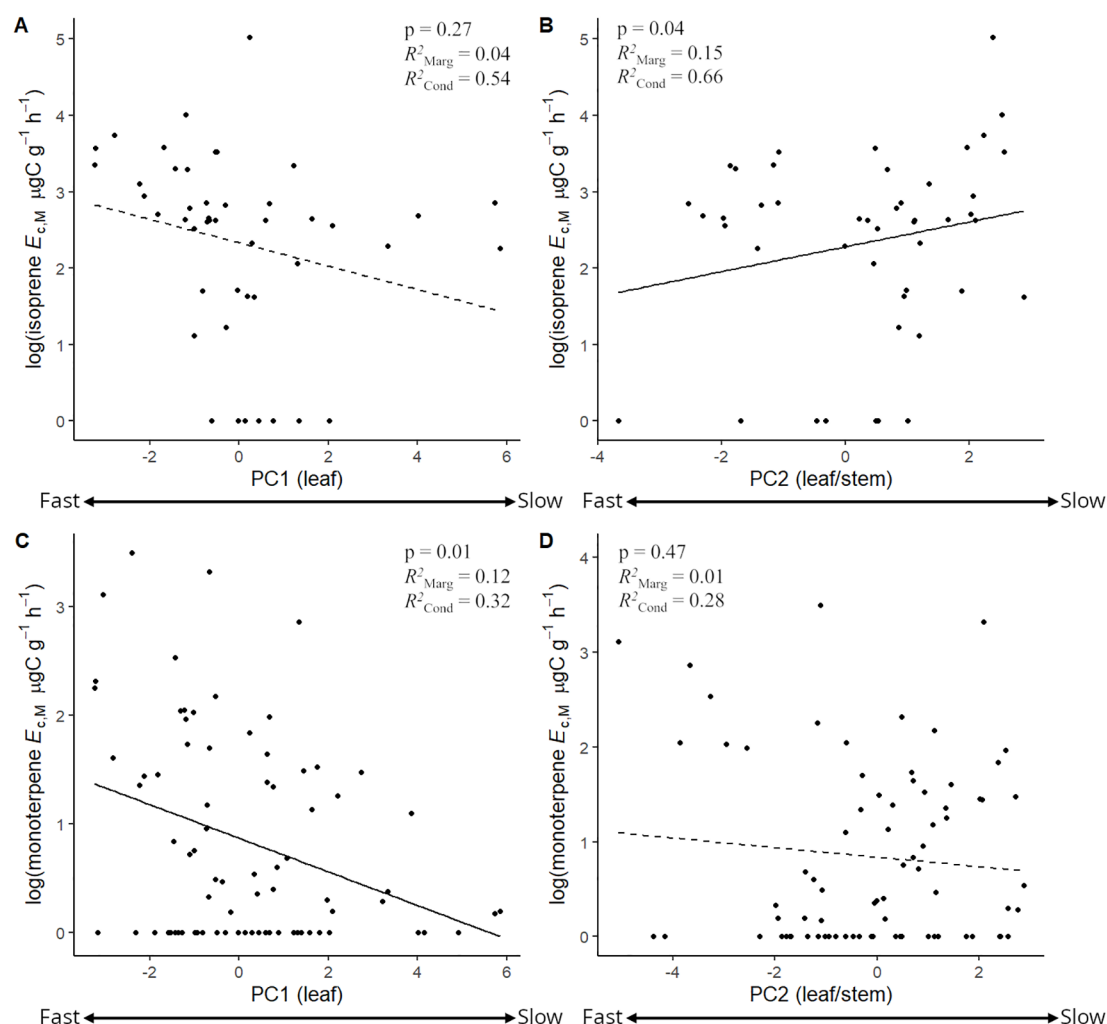
FIGURE 6
Mixed effects linear regression models between the log + 1 of isoprene emission capacity per leaf dry mass (isoprene $E_{c,M}$, µg C g^{-1} h^{-1}) and PC1 **(A)** and PC2 **(B)**, and between the log + 1 of monoterpene emission capacity per leaf dry mass (monoterpene $E_{c,M}$, µg C g^{-1} h^{-1}) and PC1 **(C)** and PC2 **(D)**. Negative and positive PC scores reflected faster and slower leaf (PC1) and leaf/stem (PC2) economics strategies, respectively. Models were performed with all trees from species that showed the capacity to emit isoprene **(A, B**, n = 43) and monoterpenes **(C, D**, n = 78) and included species as a random factor. Solid lines represent $p < 0.05$.

which highlight its involvement not only in abiotic stress tolerance but also in the modulation of defense responses (Monson et al., 2021). Therefore, it is possible that, in these Central Amazon Forest woody species, the carbon cost of isoprene production is compensated by enhanced tissue longevity and mechanical protection, supporting the hypothesis (H1b) that, for isoprene, slower-growing strategies can accommodate the metabolic costs of emissions by reinforcing plant persistence and defense capacities.

Furthermore, the fact that this second axis of mixed leaf/stem CES seemed to be more associated with the capacity to emit isoprene and also significantly predicted isoprene E_c may corroborate the view that isoprene's role is not restricted to leaf-level stress responses and that the compound has a more systemic role in the mediation of growth and defense responses in the entire tree (Monson et al., 2021). Similarly, results from pairwise standard major axis (SMA) regressions between traits from this axis in isoprene emitters may further support this idea. Parallel to this,

the observed increase in isoprene E_c with slower, more conservative leaf and stem CES may reflect an additional mechanism to cope with mild drought (Niinemets, 2010; Peñuelas and Staudt, 2010; Taylor et al., 2018), as occurs during the relatively short dry season at the ATTO site (Schmitt et al., 2023), but more research would be needed to confirm this.

On the other hand, magnitudes of monoterpene E_c significantly increased toward faster leaf CES. While the relationship between isoprene E_c and PC1 indicated a similar pattern, this was not statistically significant. In any case, isoprene and light-dependent monoterpene emissions most often incur the instantaneous use of recently assimilated photosynthetic carbon that could otherwise be allocated to respiration and growth (Delwiche and Sharkey, 1993; Affek and Yakir, 2003; Loreto et al., 2004; Huang et al., 2017; Lehmanski et al., 2024). Therefore, it is reasonable that, within isoprene and monoterpene emitters, magnitudes of E_c would increase toward faster leaves since a faster leaf metabolism - with

higher photosynthetic rates - would generally be needed to provide sufficient carbon assimilation to support higher emission rates (Loreto and Sharkey, 1990; Delwiche and Sharkey, 1993; Loreto et al., 1996; Magel et al., 2006; Sharkey and Monson, 2017). However, the relationship between leaf CES and magnitudes of isoprene E_c might be more complex, as the compound is likely associated with both growth and defense responses, and a more significant relationship between isoprene and slower leaf and stem strategies is likely smoothing the effect of faster leaf strategies in supporting higher magnitudes of isoprene E_c.

Finally, chi-squared (χ^2) analysis comparing observed and expected occurrences of isoprene and monoterpene emitters was not significant, and E_c magnitudes of trees from species that emit both compounds did not have a significant relationship. This suggests that, in central Amazon tree species, isoprene and monoterpene emissions do not vary simultaneously (Harrison et al., 2013), and the absence of a relationship between both compounds might be a result of the "opportunistic" character of their production. The presence of isoprene and terpene synthase encoding genes is, ultimately, the determinant of isoprene and monoterpene emissions (Dani et al., 2014; Loreto and Fineschi, 2015). This is emphasized by the results of mixed effects linear regression models, which showed the importance of taxonomic species in emission variation by the overall smaller marginal R-squared (R^{2Marg}) value - which represents the variance explained by fixed predictors - compared to the R-squared conditioned to the random factor (R^{2Cond}) in the models. Yet, while terpene synthases are widespread, the evolution of isoprene synthase is quite puzzling, as the capacity to emit isoprene seems to appear and disappear in plant lineages without a clear phylogenetic thread (Dani et al., 2014; Loreto and Fineschi, 2015).

However, it has been suggested that isoprene synthase has evolved from terpene synthases (Sharkey et al., 2013; Li et al., 2017). Considering the high species richness and complexity of ecological interactions observed in Amazonian tree communities (Cardoso et al., 2017; ter Steege et al., 2025), and the importance of monoterpenes for plant signaling (Gershenzon and Dudareva, 2007; Fineschi and Loreto, 2012; Xiao et al., 2012), we argue that it would be highly advantageous for an isoprene-emitting species to retain terpene synthase genes and be able to produce both compounds. Moreover, the fact that we have observed many species emitting both isoprene and monoterpenes (12 species) or only monoterpenes (15 species) versus two species that only emitted isoprene and two species that did not emit any VIs further supports this, but more research would be needed to test this hypothesis. As non-emitters of monoterpenes were rare (two species), and positioned at the faster end of leaf CES and the slower end of fast/stem CES, a deeper evaluation of possible alternate defense strategies for these species (e.g., phenolics or alkaloids) would be interesting for a future study.

Lastly, although we cannot fully disentangle slow constitutive, stress-induced, and light-dependent monoterpene emissions within our measurements, we discard the possibility of having captured heat stress-induced emissions since measurements were done at a standard leaf temperature of 30°C, which is not stressful for tropical trees (Slot and Winter, 2017). Moreover, although we could have

captured slow constitutive or even small indirect herbivory-induced emissions (Ton et al., 2006; Frost et al., 2007) triggered by herbivory/pathogens on other leaves from the measured tree or neighboring trees (Fineschi and Loreto, 2012), these would not be expected to increase with higher N_{mass} and P_{mass} (Kesselmeier and Staudt, 1999). Therefore, we argue that the relationship between increasing magnitudes of monoterpene E_c in faster leaves is probably being driven by light-dependent monoterpenes.

In that sense, we did not discuss sesquiterpene emissions in this study as they were not observed in our measurements. Likely, we did not observe sesquiterpene emissions because these derive solely from storage pools, being light-independent, and constitutive storage pool emissions at non-stressful standard conditions were possibly too low to be detected by our measurement system. Nevertheless, a parallel study did detect sesquiterpene emission rates from one tree species (*Protium hebetatum*) during the dry season (Gomes Alves et al., 2022), and brevideciduous isoprene emitters from *terra firme* showed higher diversity of stored sesquiterpene compounds and total phenolics content with increases in magnitudes of isoprene E_c (Robin et al., 2024). These studies further indicate the importance of sesquiterpene emissions in stress responses, as well as reinforce the idea that isoprene emissions possibly coordinate the supply of resources to the production of defense compounds (Monson et al., 2021).

4.3 Distribution of isoprene and monoterpene emissions

Previous synthesis studies assumed that about 20-38% of tropical woody species emitted isoprene (Harley et al., 2004; Loreto and Fineschi, 2015), but more recently, studies have revealed that this percentage can be even higher, up to 76% (Jardine et al., 2020; Mu et al., 2022). In our study, we observed the capacity to emit isoprene in 45% of the species measured, and a vast majority of species showed the capacity to emit monoterpenes (87%). Such high numbers of monoterpene emitters and emitters of both isoprene and monoterpenes reinforce the idea that monoterpene emissions were possibly preferentially selected by competitive and herbivore pressure under the great species richness and complexity of ecological interactions found in Amazonian tree communities - factors that were shown to be associated with increases in monoterpene emission rates (Kigathi et al., 2019) and in the number of monoterpene emitters (Massad et al., 2017; Sedio et al., 2017; Sun et al., 2024).

Such a great proportion of monoterpene emitters and the absence of non-monoterpene emitters in *terra firme* corroborate a consistent trend of studies revealing larger numbers of monoterpene emitters and higher monoterpene emission rates in the Amazon Forest than previously thought (Gomes Alves et al., 2022; A. B. Jardine et al., 2015; K. J. Jardine et al., 2017, 2020; Kuhn et al., 2004, 2007; Yáñez-Serrano et al., 2018). It also supports observations for a site in eastern Amazonia showing that the magnitude of monoterpene emissions could be as great as ~10% that of isoprene emissions (Sarkar et al., 2020), with even higher

proportions during the El-Niño years (Pfannerstill et al., 2018). From the perspective of forest-atmosphere interactions, monoterpenes are much more chemically reactive than isoprene, with a yield rate of secondary organic aerosol (SOA) formation that can reach ~10% (Griffin et al., 1999b, 1999a) while isoprene has been reported as <6% (Kroll et al., 2005; Xu et al., 2014), indicating the importance of putting effort into better quantifying monoterpene emissions from Amazon woody species.

4.4 Study limitations and implications for emission modeling

The numerous logistical challenges associated with conducting extensive field campaigns in the Amazon Forest - e.g., remote and hard-to-access sites, uncertainties in taxonomic classifications, difficulties in locating sufficient repetitions per species, difficulties in sampling branches from very tall trees - contributed to limitations in the numbers of available replicates per species and of leaves measured per tree. Increasing these numbers could have helped reduce the observed intra-specific variation in VI E_c magnitude, as well as potentially increase the number of species with the capacity to emit isoprene, which could have helped better elucidate the observed relationships between isoprene and fast-slow CES. In that sense, in this study, we applied resampling techniques to robustly quantify uncertainty in small sample sizes (Efron and Tibshirani, 1994), and consistently included species as a random effect in our general linear regression models to address the non-independence among observations within the same species and partition the variance attributable to species-specific effects (Bates et al., 2015).

Nonetheless, future studies should consider employing Bayesian hierarchical models with informative priors and adjusted degrees-of-freedom methods (e.g., Kenward-Roger adjustment) to better address potential biases from limited sample sizes (Kenward and Roger, 1997). We also recommend that future research should invest in the training of specialized field taxonomists and the development of more comprehensive taxonomic inventories to reduce uncertainties in species classification and increase species sample sizes. Moreover, conducting a rapid photosynthetic pre-screening among several trees of the same species can help target VI measurements to trees within a similar photosynthetic range, which has been shown as associated with a drastic reduction of intra-specific variability in VI E_c (Zeng et al., 2024).

Still, we argue that observing isoprene or monoterpene emissions in a single leaf from a single tree is sufficient to classify the species as an emitter, as emissions should be conserved at the taxonomic species level (Dani et al., 2014; Loreto and Fineschi, 2015). The primary focus of our study was to position VI emitters along CES and evaluate variations in magnitudes of VI E_c across CES. Hence, we did not formulate hypotheses for non-emitters, and we argue that a scenario where non-emissions were incorrectly attributed to potential emitters would not affect our conclusions. Furthermore, the data and results we presented here contain valuable information to motivate further investigation on how VI

emissions vary with plant functional strategies in the Amazon Forest and highlight the importance of leaf-level measurements to accurately estimate monoterpene fluxes; since measurements of monoterpene fluxes at ecosystem or canopy level usually fail to register actual emission rates due to strong photochemical oxidation of monoterpenes before they reach the above canopy (Kuhn et al., 2007; Jardine et al., 2015).

In addition, although the Amazon Forest is the largest source of VI fluxes to the global atmosphere (Guenther et al., 2012; Sindelarova et al., 2014), model estimates still carry high uncertainties because only a few observational studies with mechanistic and process-based approaches have been conducted, hindering modeling optimization (Alves et al., 2018; Yáñez-Serrano et al., 2020). Two major reasons for model uncertainties are: i) the correct determination of VI source magnitude or E_c (also known as emission factor); and ii) the determination of the tree emitter fraction of a given forest, as represented in models (e.g., MEGAN v2.1; Guenther et al., 2012) (Gomes Alves et al., 2023). For instance, MEGAN v.2 relies on very simplified schemes of plant functional type (PFT) distributions (e.g., CLM4 model), with a single E_c value for each PFT. Moreover, E_c values input in current models are generally derived either from a limited number of flux tower measurements - obtained exclusively from *terra firme* forests in the central Amazon (Alves et al., 2018; Sarkar et al., 2020; Langford et al., 2022; DiMaria et al., 2023; Gomes Alves et al., 2023) - or from flight measurements and satellite retrievals, which are often restricted to isoprene (e.g., Bauwens et al., 2016; Gu et al., 2017). In this light, this study indicates a direction to improve global VI model predictions by estimating more accurate E_c values and emitter fractions of Amazonian Forest types with the support of functional ecology.

Here, we showed that the capacity to emit and the magnitude of isoprene and monoterpene E_c differentially varied with fast-slow CES. While the capacity to emit monoterpenes was widespread throughout the whole range of CES captured in our PCA, magnitudes of monoterpene E_c significantly increased in faster leaves. Meanwhile, the capacity to emit isoprene was associated with slower leaf and stem CES, and magnitudes of isoprene E_c increased with slower leaves and stems as well. Based on our findings, we argue that, with more studies dedicated to further elucidate the relationships between plant functional strategies and VI emissions, soon we will be able to parameterize and scale up forest VI emission factors using more accurate plant functional trait distributions. This is very promising because plant functional traits are not only easier to measure than VI emissions but are also increasingly accessible through expanding open databases.

5 Conclusion

Our study presented a unique dataset of *in situ* isoprene and monoterpene E_c, and functional trait measurements for 91 trees from 31 species of angiosperm distributed across different vegetation types in the central Amazon. We saw that VI emissions were equally distributed across vegetation types, with a

surprisingly high amount of monoterpene emitters (87% of species) that showed increasing monoterpene E_c with faster leaf strategies. We also observed the capacity to emit isoprene in 45% of species, and isoprene emitters tended to be concentrated toward slower leaf and stem strategies, with isoprene E_c also significantly increasing toward slower leaves and stems. We provided a more integrated view of the relationships between VI emissions and functional traits on different organ-system levels and a direction for new studies to improve modeled emission estimates based on forest functional compositions. Our study adds a new piece to the development of a more biologically robust way of estimating plant VI emissions and reducing model uncertainties; this is particularly critical in highly biodiverse environments such as the Amazon Forest, which are considered the main source of VIs to the global atmosphere.

Data availability statement

The dataset presented in this study is available at: https://doi.org/10.17871/ATTO.364.8.1600.

Author contributions

MR: Conceptualization, Data curation, Formal Analysis, Investigation, Methodology, Project administration, Resources, Software, Validation, Visualization, Writing – original draft, Writing – review & editing. EG: Conceptualization, Data curation, Formal Analysis, Funding acquisition, Investigation, Methodology, Project administration, Resources, Software, Supervision, Validation, Visualization, Writing – original draft, Writing – review & editing. TT: Conceptualization, Data curation, Investigation, Validation, Visualization, Writing – original draft, Writing – review & editing. DP: Data curation, Investigation, Visualization, Writing – original draft, Writing – review & editing. SD: Conceptualization, Data curation, Formal Analysis, Methodology, Resources, Software, Writing – original draft, Writing – review & editing. JG: Methodology, Resources, Software, Writing – original draft, Writing – review & editing. JoS: Data curation, Methodology, Writing – original draft, Writing – review & editing. FW: Data curation, Methodology, Writing – original draft, Writing – review & editing. MP: Data curation, Methodology, Writing – original draft, Writing – review & editing. ST: Conceptualization, Funding acquisition, Resources, Writing – original draft, Writing – review & editing. JuS: Conceptualization, Data curation, Formal Analysis, Investigation, Methodology, Project administration, Resources, Supervision, Validation, Visualization, Writing – original draft, Writing – review & editing.

Funding

Acknowledgments

Conflict of interest

The authors declare that the research was conducted in the absence of any commercial or financial relationships that could be construed as a potential conflict of interest.

Generative AI statement

The author(s) declare that no Generative AI was used in the creation of this manuscript.

Publisher's note

All claims expressed in this article are solely those of the authors and do not necessarily represent those of their affiliated organizations, or those of the publisher, the editors and the reviewers. Any product that may be evaluated in this article, or claim that may be made by its manufacturer, is not guaranteed or endorsed by the publisher.

Supplementary material

The Supplementary Material for this article can be found online at: https://www.frontiersin.org/articles/10.3389/fpls.2025.1561316/full#supplementary-material

References

Affek, H. P., and Yakir, D. (2003). Natural abundance carbon isotope composition of isoprene reflects incomplete coupling between isoprene synthesis and photosynthetic carbon flow. *Plant Physiol.* 131, 1727–1736. doi: 10.1104/PP.102.012294

Albert, L. P., Wu, J., Prohaska, N., de Camargo, P. B., Huxman, T. E., Tribuzy, E. S., et al. (2018). Age-dependent leaf physiology and consequences for crown-scale carbon uptake during the dry season in an Amazon evergreen forest. *New Phytol.* 219, 870–884. doi: 10.1111/nph.15056

Alves, E. G., Harley, P., Gonçalves, J.F.de C., Moura, C.E.da S., and Jardine, K. (2014). Effects of light and temperature on isoprene emission at different leaf developmental stages of eschweilera coriacea in central Amazon. *Acta Amazon* 44, 9–18. doi: 10.1590/S0044-59672014000100002

Alves, E. G., Jardine, K., Tota, J., Jardine, A., Maria Yãnez-Serrano, A., Karl, T., et al. (2016). Seasonality of isoprenoid emissions from a primary rainforest in central Amazonia. *Atmos Chem. Phys.* 16, 3903–3925. doi: 10.5194/acp-16-3903-2016

Alves, E. G., Tóta, J., Turnipseed, A., Guenther, A., Vega Bustillos, J. O. W., Santana, R. A., et al. (2018). Leaf phenology as one important driver of seasonal changes in isoprene emissions in central Amazonia. *Biogeosciences* 15, 4019–4032. doi: 10.5194/bg-15-4019-2018

Andreae, M. O., Acevedo, O. C., Araùjo, A., Artaxo, P., Barbosa, C. G. G., Barbosa, H. M. J., et al. (2015). The Amazon Tall Tower Observatory (ATTO): overview of pilot measurements on ecosystem ecology, meteorology, trace gases, and aerosols. *Atmos Chem. Phys.* 15, 10723–10776. doi: 10.5194/acp-15-10723-2015

Arneth, A., and Niinemets, Ü. (2010). Induced BVOCs: how to bug our models? *Trends Plant Sci.* 15, 118–125. doi: 10.1016/j.tplants.2009.12.004

Asner, G. P., Martin, R. E., Tupayachi, R., Anderson, C. B., Sinca, F., Carranza-Jiménez, L., et al. (2014). Amazonian functional diversity from forest canopy chemical assembly. *Proc. Natl. Acad. Sci. U S A* 111, 5604–5609. doi: 10.1073/pnas.1401181111

Bamberger, I., Ruehr, N. K., Schmitt, M., Gast, A., Wohlfahrt, G., and Arneth, A. (2017). Isoprene emission and photosynthesis during heat waves and drought in black locust. *Biogeosciences discussions* 14, 3649. doi: 10.5194/BG-2017-32

Baraloto, C., Paine, C. E. T., Poorter, L., Beauchene, J., Bonal, D., Domenach, A. M., et al. (2010a). Decoupled leaf and stem economics in rain forest trees. *Ecol. Lett.* 13, 1338–1347. doi: 10.1111/j.1461-0248.2010.01517.x

Baraloto, C., Timothy Paine, C. E., Patiño, S., Bonal, D., Hérault, B., and Chave, J. (2010b). Functional trait variation and sampling strategies in species-rich plant communities. *Funct. Ecol.* 24, 208–216. doi: 10.1111/j.1365-2435.2009.01600.x

Bates, D., Maechler, M., Bolker, B., and Walker, S. (2015). Fitting linear mixed-effects models using lme4. *J. Stat. Software* 67, 1–48. doi: 10.18637/jss.v067.i01

Bauwens, M., Stavrakou, T., Müller, J.-F., De Smedt, I., Van Roozendael, M., van der Werf, G. R., et al. (2016). Nine years of global hydrocarbon emissions based on source inversion of OMI formaldehyde observations. *Atmos Chem. Phys.* 16, 10133–10158. doi: 10.5194/acp-16-10133-2016

Behnke, K., Ehlting, B., Teuber, M., Bauerfeind, M., Louis, S., Hänsch, R., et al. (2007). Transgenic, non-isoprene emitting poplars don't like it hot. *Plant J.* 51, 485–499. doi: 10.1111/j.1365-313X.2007.03157.x

Behnke, K., Kaiser, A., Zimmer, I., Brüggemann, N., Janz, D., Polle, A., et al. (2010). RNAi-mediated suppression of isoprene emission in poplar transiently impacts phenolic metabolism under high temperature and high light intensities: A transcriptomic and metabolomic analysis. *Plant Mol. Biol.* 74, 61–75. doi: 10.1007/S11103-010-9654-Z/FIGURES/7

Bourtsoukidis, E., Pozzer, A., Williams, J., Makowski, D., Peñuelas, J., Matthaios, V. N., et al. (2024). High temperature sensitivity of monoterpene emissions from global vegetation. *Commun. Earth Environ.* 5, 1–10. doi: 10.1038/s43247-023-01175-9

Byron, J., Kreuzwieser, J., Purser, G., van Haren, J., Ladd, S. N., Meredith, L. K., et al. (2022). Chiral monoterpenes reveal forest emission mechanisms and drought responses. *Nature* 609, 307–312. doi: 10.1038/s41586-022-05020-5

Cardoso, D., Särkinen, T., Alexander, S., Amorim, A. M., Bittrich, V., Celis, M., et al. (2017). Amazon plant diversity revealed by a taxonomically verified species list. *Proc. Natl. Acad. Sci. U S A* 114, 10695–10700. doi: 10.1073/pnas.1706756114

Chauvel, A., Lucas, Y., and Boulet, R. (1987). On the genesis of the soil mantle of the region of Manaus, Central Amazonia, Brazil. *Experientia* 43, 234–241. doi: 10.1007/BF01945546

Chave, J., Coomes, D., Jansen, S., Lewis, S. L., Swenson, N. G., and Zanne, A. E. (2009). Towards a worldwide wood economics spectrum. *Ecol. Lett.* 12, 351–366. doi: 10.1111/j.1461-0248.2009.01285.x

Chazdon, R. L., and Fetcher, N. (1984). Photosynthetic light environments in a lowland tropical rain forest in Costa Rica. *J. Ecol.* 72, 553–564. doi: 10.2307/2260066

Cosme, L. H. M., Schietti, J., Costa, F. R. C., and Oliveira, R. S. (2017). The importance of hydraulic architecture to the distribution patterns of trees in a central Amazonian forest. *New Phytol.* 215, 113–125. doi: 10.1111/nph.14508

Costa, F. R. C., Lang, C., Almeida, D. R. A., Castilho, C. V., and Poorter, L. (2018). Near-infrared spectrometry allows fast and extensive predictions of functional traits from dry leaves and branches. *Ecol. Appl.* 28, 1157–1167. doi: 10.1002/eap.1728

Costa, F. R. C., Schietti, J., Stark, S. C., and Smith, M. N. (2023). The other side of tropical forest drought: do shallow water table regions of Amazonia act as large-scale hydrological refugia from drought? *New Phytol.* 237, 714–733. doi: 10.1111/nph.17914

Dani, K. G. S., Jamie, I. M., Prentice, I. C., and Atwell, B. J. (2014). Evolution of isoprene emission capacity in plants. *Trends Plant Sci.* 19, 439–446. doi: 10.1016/j.tplants.2014.01.009

Dani, K. G. S., Pollastri, S., Pinosio, S., Reichelt, M., Sharkey, T. D., Schnitzler, J. P., et al. (2022). Isoprene enhances leaf cytokinin metabolism and induces early senescence. *New Phytol.* 234, 961–974. doi: 10.1111/nph.17833

Déjardin, A., Laurans, F., Arnaud, D., Breton, C., Pilate, G., and Leplé, J. C. (2010). Wood formation in angiosperms. *C R Biol.* 333, 325–334. doi: 10.1016/J.CRVI.2010.01.010

Delwiche, C. F., and Sharkey, T. D. (1993). Rapid appearance of 13C in biogenic isoprene when 13CO2 is fed to intact leaves. *Plant Cell Environ.* 16, 587–591. doi: 10.1111/j.1365-3040.1993.tb00907.x

Demarchi, L. O., Klein, V. P., Aguiar, D. P. P., Marinho, L. C., Ferreira, M. J., Lopes, A., et al. (2022). The specialized white-sand flora of the Uatumã Sustainable Development Reserve, central Amazon, Brazil. *Check List* 18, 187–217. doi: 10.15560/18.1.187

Díaz, S., Kattge, J., Cornelissen, J. H. C., Wright, I. J., Lavorel, S., Dray, S., et al. (2016). The global spectrum of plant form and function. *Nature* 529, 167–171. doi: 10.1038/nature16489

DiMaria, C. A., Jones, D. B. A., Worden, H., Bloom, A. A., Bowman, K., Stavrakou, T., et al. (2023). Optimizing the isoprene emission model MEGAN with satellite and ground-based observational constraints. *J. Geophysical Res.: Atmospheres* 128. doi: 10.1029/2022JD037822

Efron, B., and Tibshirani, R. J. (1994). An introduction to the bootstrap. Published. *Monographs on Statistics and Applied Probability 57.* Taylor & Francis Group: Boca Raton, FL, United States.

Empresa Brasileira de Pesquisa Agropecuária (1999). *Manual de análise química de solos, plantas e fertilizantes* (Brasília, Brazil: EMBRAPA).

Fernández-Martínez, M., Llusià, J., Filella, I., Niinemets, Ü., Arneth, A., Wright, I. J., et al. (2018). Nutrient-rich plants emit a less intense blend of volatile isoprenoids. *New Phytol.* 220, 773–784. doi: 10.1111/nph.14889

Fineschi, S., and Loreto, F. (2012). Leaf volatile isoprenoids: An important defensive armament in forest tree species. *IForest* 5, 13–17. doi: 10.3832/ifor0607-009

Frank, L., Wenig, M., Ghirardo, A., van der Krol, A., Vlot, A. C., Schnitzler, J. P., et al. (2021). Isoprene and β-caryophyllene confer plant resistance via different plant internal signalling pathways. *Plant Cell Environ.* 44, 1151–1164. doi: 10.1111/pce.14010

Frost, C. J., Appel, H. M., Carlson, J. E., De Moraes, C. M., Mescher, M. C., and Schultz, J. C. (2007). Within-plant signalling via volatiles overcomes vascular constraints on systemic signalling and primes responses against herbivores. *Ecol. Lett.* 10, 490–498. doi: 10.1111/j.1461-0248.2007.01043.x

Gershenzon, J., and Dudareva, N. (2007). The function of terpene natural products in the natural world. *Nat. Chem. Biol.* 3, 408–414. doi: 10.1038/nchembio.2007.5

Ghirardo, A., Xie, J., Zheng, X., Wang, Y., Grote, R., Block, K., et al. (2016). Urban stress-induced biogenic VOC emissions and SOA-forming potentials in Beijing. *Atmos Chem. Phys.* 16, 2901–2920. doi: 10.5194/ACP-16-2901-2016

Gomes Alves, E., Aquino Santana, R., Quaresma Dias-Júnior, C., Botía, S., Taylor, T., Yáñez-Serrano, A. M., et al. (2023). Intra- and interannual changes in isoprene emission from central Amazonia. *Atmos Chem. Phys.* 23, 8149–8168. doi: 10.5194/acp-23-8149-2023

Gomes Alves, E., Taylor, T., Robin, M., Pinheiro Oliveira, D., Schietti, J., Duvoisin Júnior, S., et al. (2022). Seasonal shifts in isoprenoid emission composition from three hyperdominant tree species in central Amazonia. *Plant Biol.* 24, 721–733. doi: 10.1111/plb.13419

Griffin, R. J., Cocker, D. R., Flagan, R. C., and Seinfeld, J. H. (1999a). Organic aerosol formation from the oxidation of biogenic hydrocarbons. *J. Geophysical Res.: Atmospheres* 104, 3555–3567. doi: 10.1029/1998JD100049

Griffin, R. J., Cocker, D. R., Seinfeld, J. H., and Dabdub, D. (1999b). Estimate of global atmospheric organic aerosol from oxidation of biogenic hydrocarbons. *Geophys. Res. Lett.* 26, 2721–2724. doi: 10.1029/1999GL900476

Gu, D., Guenther, A. B., Shilling, J. E., Yu, H., Huang, M., Zhao, C., et al. (2017). Airborne observations reveal elevational gradient in tropical forest isoprene emissions. *Nat. Commun.* 8. doi: 10.1038/ncomms15541

Guenther, A., Jiang, X., Heald, C. L., Sakulyanontvittaya, T., Duhl, T., Emmons, L. K., et al. (2012). The Model of Emissions of Gases and Aerosols from Nature version 2.1 (MEGAN2.1): an extended and updated framework for modeling biogenic emissions. *Geosci. Model Dev.* 5, 1471–1492. doi: 10.5194/gmd-5-1471-2012

Guenther, A., Karl, T., Harley, P., Wiedinmyer, C., Palmer, P. I., and Geron, C. (2006). Estimates of global terrestrial isoprene emissions using MEGAN (Model of Emissions of Gases and Aerosols from Nature). *Atmos Chem. Phys.* 6, 3181–3210. doi: 10.5194/acp-6-3181-2006

Hacke, U. G., Sperry, J. S., Pockman, W. T., Davis, S. D., and McCulloh, K. A. (2001). Trends in wood density and structure are linked to prevention of xylem implosion by negative pressure. *Oecologia* 126, 457–461. doi: 10.1007/S004420100628/METRICS

Harley, P., Vasconcellos, P., Vierling, L., Pinheiro, C. C. D. S., Greenberg, J., Guenther, A., et al. (2004). Variation in potential for isoprene emissions among Neotropical forest sites. *Glob. Chang. Biol.* 10, 630–650. doi: 10.1111/j.1529-8817.2003.00760.x

Harrison, S. P., Morfopoulos, C., Dani, K. G. S., Prentice, I. C., Arneth, A., Atwell, B. J., et al. (2013). Volatile isoprenoid emissions from plastid to planet. *New Phytol.* 197, 49–57. doi: 10.1111/nph.12021

Harvey, C. M., Li, Z., Tjellström, H., Blanchard, G. J., and Sharkey, T. D. (2015). Concentration of isoprene in artificial and thylakoid membranes. *J. Bioenerg. Biomembr.* 47, 419–429. doi: 10.1007/s10863-015-9625-9

Harvey, C. M., and Sharkey, T. D. (2016). Exogenous isoprene modulates gene expression in unstressed Arabidopsis thaliana plants. *Plant Cell Environ.* 39, 1251–1263. doi: 10.1111/PCE.12660

Hendry, G. A. F., and Grime, J. P. (1993). *Methods in comparative plant ecology: A laboratory manual* (London, UK: Chapman and Hall).

Hetherington, A. M., and Woodward, F. I. (2003). The role of stomata in sensing and driving environmental change. *Nature* 424, 901–908. doi: 10.1038/nature01843

Hoffmann, W. A., Marchin, R. M., Abit, P., and Lau, O. L. (2011). Hydraulic failure and tree dieback are associated with high wood density in a temperate forest under extreme drought. *Glob. Chang. Biol.* 17, 2731–2742. doi: 10.1111/J.1365-2486.2011.02401.X

Huang, J., Hammerbacher, A., Forkelová, L., and Hartmann, H. (2017). Release of resource constraints allows greater carbon allocation to secondary metabolites and storage in winter wheat. *Plant Cell Environ.* 40, 672–685. doi: 10.1111/pce.12885

Jardine, A. B., Jardine, K. J., Fuentes, J. D., Martin, S. T., Martins, G., Durgante, F., et al. (2015). Highly reactive light-dependent monoterpenes in the Amazon. *Geophys. Res. Lett.* 42, 1576–1583. doi: 10.1002/2014GL062573

Jardine, K. J., Jardine, A. B., Holm, J. A., Lombardozzi, D. L., Negron-Juarez, R. I., Martin, S. T., et al. (2017). Monoterpene 'thermometer' of tropical forest-atmosphere response to climate warming. *Plant Cell Environ.* 40, 441–452. doi: 10.1111/pce.12879

Jardine, K. J., Zorzanelli, R. F., Gimenez, B. O., Oliveira Piva, L. R., Teixeira, A., Fontes, C. G., et al. (2020). Leaf isoprene and monoterpene emission distribution across hyperdominant tree genera in the Amazon basin. *Phytochemistry* 175, 112366. doi: 10.1016/j.phytochem.2020.112366

Johansen, D. A. (1940). *Plant microtechnique* (New York, USA: McGraw Hill Book).

Joo, Y., Schuman, M. C., Goldberg, J. K., Kim, S. G., Yon, F., Brütting, C., et al. (2018). Herbivore-induced volatile blends with both "fast" and "slow" components provide robust indirect defence in nature. *Funct. Ecol.* 32, 136–149. doi: 10.1111/1365-2435.12947

Kattge, J., Díaz, S., Lavorel, S., Prentice, I. C., Leadley, P., Bönisch, G., et al. (2011). TRY - a global database of plant traits. *Glob. Chang. Biol.* 17, 2905–2935. doi: 10.1111/j.1365-2486.2011.02451.x

Keenan, T. F., and Niinemets, Ü. (2016). Global leaf trait estimates biased due to plasticity in the shade. *Nat. Plants* 3. doi: 10.1038/nplants.2016.201

Keller, M., and Lerdau, M. (1999). Isoprene emission from tropical forest canopy leaves. *Global Biogeochem. Cycles* 13, 19–29. doi: 10.1029/1998GB900007

Kenward, M. G., and Roger, J. H. (1997). Small sample inference for fixed effects from restricted maximum likelihood. *Biometrics* 53, 983. doi: 10.2307/2533558

Kesselmeier, J., and Staudt, M. (1999). Biogenic volatile organic compounds (VOC): an overview on emission, physiology and ecology. *J. Atmospheric Chem.* 33, 23–88. doi: 10.1023/A:1006127516791

Kigathi, R. N., Weisser, W. W., Reichelt, M., Gershenzon, J., and Unsicker, S. B. (2019). Plant volatile emission depends on the species composition of the neighboring plant community. *BMC Plant Biol.* 19. doi: 10.1186/s12870-018-1541-9

Kroll, J. H., Ng, N. L., Murphy, S. M., Flagan, R. C., and Seinfeld, J. H. (2005). Secondary organic aerosol formation from isoprene photooxidation under high-NOx conditions. *Geophys. Res. Lett.* 32, n/a–n/a. doi: 10.1029/2005GL023637

Kuhn, U., Andreae, M. O., Ammann, C., Araújo, A. C., Brancaleoni, E., Ciccioli, P., et al. (2007). Isoprene and monoterpene fluxes from Central Amazonian rainforest inferred from tower-based and airborne measurements, and implications on the atmospheric chemistry and the local carbon budget. *Atmos Chem. Phys.* 7, 2855–2879. doi: 10.5194/acp-7-2855-2007

Kuhn, U., Rottenberger, S., Biesenthal, T., Wolf, A., Schebeske, G., Ciccioli, P., et al. (2004). Seasonal differences in isoprene and light-dependent monoterpene emission by Amazonian tree species. *Glob. Chang. Biol.* 10, 663–682. doi: 10.1111/j.1529-8817.2003.00771.x

Kulmala, M., Nieminen, T., Chellapermal, R., Makkonen, R., Bäck, J., and Kerminen, V.-M. (2013). *Climate feedbacks linking the increasing atmospheric CO2 concentration, BVOC emissions, aerosols and clouds in forest ecosystems.* 489–508. doi: 10.1007/978-94-007-6606-8_17

Langford, B., House, E., Valach, A., Hewitt, C. N., Artaxo, P., Barkley, M. P., et al. (2022). Seasonality of isoprene emissions and oxidation products above the remote Amazon. *Environ. Sci.: Atmospheres* 2, 230–240. doi: 10.1039/D1EA00057H

Lantz, A. T., Allman, J., Weraduwage, S. M., and Sharkey, T. D. (2019). Isoprene: New insights into the control of emission and mediation of stress tolerance by gene expression. *Plant Cell Environ.* 42, 2808–2826. doi: 10.1111/pce.13629

Laothawornkitkul, J., Paul, N. D., Vickers, C. E., Possell, M., Taylor, J. E., Mullineaux, P. M., et al. (2008). Isoprene emissions influence herbivore feeding decisions. *Plant Cell Environ.* 31, 1410–1415. doi: 10.1111/j.1365-3040.2008.01849.x

Laule, O., Fürholz, A., Chang, H. S., Zhu, T., Wang, X., Heifetz, P. B., et al. (2003). Crosstalk between cytosolic and plastidial pathways of isoprenoid biosynthesis in Arabidopsis thaliana. *Proc. Natl. Acad. Sci. U S A* 100, 6866–6871. doi: 10.1073/PNAS.1031755100/SUPPL_FILE/1755FIG4.JPG

Legner, N., Fleck, S., Leuschner, C., and Fleck, S. (2014). Within-canopy variation in photosynthetic capacity, SLA and foliar N in temperate broad-leaved trees with contrasting shade tolerance. *Trees* 28, 263–280. doi: 10.1007/s00468-013-0947-0

Lehmanski, L. M. A., Kösters, L. M., Huang, J., Göbel, M., Gershenzon, J., and Hartmann, H. (2024). Windthrow causes declines in carbohydrate and phenolic concentrations and increased monoterpene emission in Norway spruce. *PloS One* 19, e0302714. doi: 10.1371/JOURNAL.PONE.0302714

Lehning, A., Zimmer, I., Steinbrecher, R., Brüggemann, N., and Schnitzler, J.-P. (1999). Isoprene synthase activity and its relation to isoprene emission in Quercus robur L. leaves. *Plant Cell Environ.* 22, 495–504. doi: 10.1046/j.1365-3040.1999.00425.x

Lenth, R. (2024). *emmeans: estimated marginal means, aka least-squares means* (R package version 1.10.1). Available at: https://CRAN.R-project.org/package=emmeans.

Li, M., Xu, J., Algarra Alarcon, A., Carlin, S., Barbaro, E., Cappellin, L., et al. (2017). In planta recapitulation of isoprene synthase evolution from ocimene synthases. *Mol. Biol. Evol.* 34, 2583–2599. doi: 10.1093/molbev/msx178

Llusia, J., Sardans, J., Niinemets, Ü., Owen, S. M., and Peñuelas, J. (2014). A screening study of leaf terpene emissions of 43 rainforest species in Danum Valley Conservation Area (Borneo) and their relationships with chemical and morphological leaf traits. *Plant Biosyst.* 148, 307–317. doi: 10.1080/11263504.2013.770803

Lopes, A. P., Nelson, B. W., Wu, J., Graça, P. M. L., de, A., Tavares, J. V., et al. (2016). Leaf flush drives dry season green-up of the Central Amazon. *Remote Sens Environ.* 182, 90–98. doi: 10.1016/J.RSE.2016.05.009

Loreto, F., Ciccioli, P., Cecinato, A., Brancaleoni, E., Frattoni, M., Fabozzi, C., et al. (1996). Evidence of the photosynthetic origin of monoterpenes emitted by quercus ilex L. Leaves by 13C labeling. *Plant Physiol.* 110, 1317–1322. doi: 10.1104/pp.110.4.1317

Loreto, F., and Fineschi, S. (2015). Reconciling functions and evolution of isoprene emission in higher plants. *New Phytol.* 206, 578–582. doi: 10.1111/nph.13242

Loreto, F., Pinelli, P., Brancaleoni, E., and Ciccioli, P. (2004). 13C labeling reveals chloroplastic and extrachloroplastic pools of dimethylallyl pyrophosphate and their contribution to isoprene formation. *Plant Physiol.* 135, 1903. doi: 10.1104/PP.104.039537

Loreto, F., and Schnitzler, J. P. (2010). Abiotic stresses and induced BVOCs. *Trends Plant Sci.* 15, 154–166. doi: 10.1016/j.tplants.2009.12.006

Loreto, F., and Sharkey, T. D. (1990). A gas-exchange study of photosynthesis and isoprene emission in Quercus rubra L. *Planta* 182, 523–531. doi: 10.1007/BF02341027/METRICS

Magel, E., Mayrhofer, S., Muïler, A., Zimmer, I., Hampp, R., and Schnitzler, J.-P. (2006). Photosynthesis and substrate supply for isoprene biosynthesis in poplar leaves. *Atmos Environ.* 40, 138–151. doi: 10.1016/j.atmosenv.2005.09.091

Martin, R. E., Asner, G. P., Bentley, L. P., Shenkin, A., Salinas, N., Huaypar, K. Q., et al. (2020). Covariance of sun and shade leaf traits along a tropical forest elevation gradient. *Front. Plant Sci.* 10. doi: 10.3389/FPLS.2019.01810/FULL

Massad, T. J., Martins de Moraes, M., Philbin, C., Oliveira, C., Cebrian Torrejon, G., Fumiko Yamaguchi, L., et al. (2017). Similarity in volatile communities leads to increased herbivory and greater tropical forest diversity. *Ecol. (Ecological Soc. America)* 98(7), 1750–1756. doi: 10.1002/ecy.1875

Monson, R. K., Harley, P. C., Litvak, M. E., Wildermuth, M., Guenther, A. B., Zimmerman, P. R., et al. (1994). Environmental and developmental controls over the seasonal pattern of isoprene emission from aspen leaves. *Oecologia* 99, 260–270. doi: 10.1007/BF00627738

Monson, R. K., Neice, A. A., Trahan, N. A., Shiach, I., McCorkel, J. T., and Moore, D. J. P. (2016). Interactions between temperature and intercellular CO2 concentration in controlling leaf isoprene emission rates. *Plant Cell Environ.* 39, 2404–2413. doi: 10.1111/pce.12787

Monson, R. K., Weraduwage, S. M., Rosenkranz, M., Schnitzler, J. P., and Sharkey, T. D. (2021). Leaf isoprene emission as a trait that mediates the growth-defense tradeoff in the face of climate stress. *Oecologia* 197, 885–902. doi: 10.1007/s00442-020-04813-7

Monson, R. K., Winkler, B., Rosenstiel, T. N., Block, K., Merl-Pham, J., Strauss, S. H., et al. (2020). High productivity in hybrid-poplar plantations without isoprene emission to the atmosphere. *Proc. Natl. Acad. Sci. U S A* 117, 1596–1605. doi: 10.1073/PNAS.1912327117

Montgomery, R. A., and Chazdon, R. L. (2001). Forest structure, canopy architecture, and light transmittance in tropical wet forests. *Ecology* 82, 2707–2718. doi: 10.1890/0012-9658(2001)082[2707:FSCAAL]2.0.CO;2

Morfopoulos, C., Prentice, I. C., Keenan, T. F., Friedlingstein, P., Medlyn, B. E., Peñuelas, J., et al. (2013). A unifying conceptual model for the environmental responses of isoprene emissions from plants. *Ann. Bot.* 112, 1223–1238. doi: 10.1093/aob/mct206

Morfopoulos, C., Sperlich, D., Peñuelas, J., Filella, I., Llusià, J., Medlyn, B. E., et al. (2014). A model of plant isoprene emission based on available reducing power captures responses to atmospheric CO2. *New Phytol.* 203, 125–139. doi: 10.1111/nph.12770

Mu, Z., Llusià, J., Zeng, J., Zhang, Y., Asensio, D., Yang, K., et al. (2022). An overview of the isoprenoid emissions from tropical plant species. *Front. Plant Sci.* 13. doi: 10.3389/fpls.2022.833030

Nagalingam, S., Seco, R., Kim, S., and Guenther, A. (2023). Heat stress strongly induces monoterpene emissions in some plants with specialized terpenoid storage structures. *Agric. For Meteorol.* 333, 109400. doi: 10.1016/j.agrformet.2023.109400

Niinemets, Ü. (2010). Mild versus severe stress and BVOCs: thresholds, priming and consequences. *Trends Plant Sci.* 15, 145–153. doi: 10.1016/j.tplants.2009.11.008

Niinemets, Ü., Kännaste, A., and Copolovici, L. (2013). Quantitative patterns between plant volatile emissions induced by biotic stresses and the degree of damage. *Front. Plant Sci.* 4. doi: 10.3389/fpls.2013.00262

Owen, S. M., and Peñuelas, J. (2005). Opportunistic emissions of volatile isoprenoids. *Trends Plant Sci.* 10, 420–426. doi: 10.1016/j.tplants.2005.07.010

Owen, S. M., and Peñuelas, J. (2013). Volatile isoprenoid emission potentials are correlated with essential isoprenoid concentrations in five plant species. *Acta Physiol. Plant* 35, 3109–3125. doi: 10.1007/S11738-013-1344-4/FIGURES/5

Peñuelas, J., and Staudt, M. (2010). BVOCs and global change. *Trends Plant Sci.* 15, 133–144. doi: 10.1016/j.tplants.2009.12.005

Pérez-Harguindeguy, N., Díaz, S., Garnier, E., Lavorel, S., Poorter, H., Jaureguiberry, P., et al. (2013). New handbook for standardised measurement of plant functional traits worldwide. *Aust. J. Bot.* 61, 167–234. doi: 10.1071/BT12225

Pfannerstill, E. Y., Nölscher, A. C., Yáñez-Serrano, A. M., Bourtsoukidis, E., Keßel, S., Janssen, R. H. H., et al. (2018). Total OH reactivity changes over the amazon rainforest during an el niño event. *Front. Forests Global Change* 1. doi: 10.3389/ffgc.2018.00012

Pfautsch, S., Macfarlane, C., Ebdon, N., and Meder, R. (2012). Assessing sapwood depth and wood properties in Eucalyptus and Corymbia spp. using visual methods and near infrared spectroscopy (NIR). *Trees - Structure Funct.* 26, 963–974. doi: 10.1007/S00468-011-0674-3/FIGURES/4

Pichersky, E., and Gershenzon, J. (2002). The formation and function of plant volatiles: perfumes for pollinator attraction and defense. *Curr. Opin. Plant Biol.* 5, 237–243. doi: 10.1016/S1369-5266(02)00251-0

Pollastri, S., Baccelli, I., and Loreto, F. (2021). Isoprene: an antioxidant itself or a molecule with multiple regulatory functions in plants? *Antioxidants* 10, 684. doi: 10.3390/ANTIOX10050684

Pollastri, S., Jorba, I., Hawkins, T. J., Llusià, J., Michelozzi, M., Navajas, D., et al. (2019). Leaves of isoprene-emitting tobacco plants maintain PSII stability at high temperatures. *New Phytol.* 223, 1307–1318. doi: 10.1111/nph.15847

Pollastri, S., Tsonev, T., and Loreto, F. (2014). Isoprene improves photochemical efficiency and enhances heat dissipation in plants at physiological temperatures. *J. Exp. Bot.* 65, 1565–1570. doi: 10.1093/JXB/ERU033

Poorter, L., Castilho, C. V., Schietti, J., Oliveira, R. S., and Costa, F. R. C. (2018). Can traits predict individual growth performance? A test in a hyperdiverse tropical forest. *New Phytol.* 219, 109–121. doi: 10.1111/nph.15206

Poorter, L., McDonald, I., Alarcón, A., Fichtler, E., Licona, J. C., Peña-Claros, M., et al. (2010). The importance of wood traits and hydraulic conductance for the performance and life history strategies of 42 rainforest tree species. *New Phytol.* 185, 481–492. doi: 10.1111/J.1469-8137.2009.03092.X

Pöschl, U., Martin, S. T., Sinha, B., Chen, Q., Gunthe, S. S., Huffman, J. A., et al. (2010). Rainforest aerosols as biogenic nuclei of clouds and precipitation in the amazon. *Sci. (1979)* 329, 1513–1516. doi: 10.1126/science.1191056

Programa de Pesquisa em Biodiversidade (PPBio) (2012). Repositório de Dados de Estudos Ecológicos. Available online at: http://ppbio.inpa.gov.br/repositorio/dados (Accessed August 23, 2018).

Quesada, C. A., Lloyd, J., Anderson, L. O., Fyllas, N. M., Schwarz, M., and Czimczik, C. I. (2011). Soils of Amazonia with particular reference to the RAINFOR sites. *Biogeosciences* 8, 1415–1440. doi: 10.5194/bg-8-1415-2011

Quiñonez-Piñón, M. R., and Valeo, C. (2018). Assessing the translucence and color-change methods for estimating sapwood depth in three boreal species. *Forests* 9, 686. doi: 10.3390/F9110686

Rasulov, B., Talts, E., and Niinemets, Ü. (2019). A novel approach for real-time monitoring of leaf wounding responses demonstrates unprecedently fast and high emissions of volatiles from cut leaves. *Plant Sci.* 283, 256–265. doi: 10.1016/j.plantsci.2019.03.006

R Core Team (2023). *R: a language and environment for statistical computing, version 4.3.2* (Vienna, Austria: R Foundation for Statistical Computing). Available at: https://www.R-project.org/.

Reich, P. B. (2014). The world-wide "fast-slow" plant economics spectrum: A traits manifesto. *J. Ecol.* 102, 275–301. doi: 10.1111/1365-2745.12211

Robin, M., Römermann, C., Niinemets, Ü., Gershenzon, J., Huang, J., Nelson, B. W., et al. (2024). Interactions between leaf phenological type and functional traits drive variation in isoprene emissions in central Amazon Forest trees. *Front. Plant Sci.* 15. doi: 10.3389/fpls.2024.1522606

Rodrigues, T. B., Baker, C. R., Walker, A. P., McDowell, N., Rogers, A., Higuchi, N., et al. (2020). Stimulation of isoprene emissions and electron transport rates as key

mechanisms of thermal tolerance in the tropical species Vismia guianensis. *Glob. Chang. Biol.* 26, 5928–5941. doi: 10.1111/gcb.15213

Sack, L., and Buckley, T. N. (2016). The developmental basis of stomatal density and flux. *Plant Physiol.* 171, 2358–2363. doi: 10.1104/pp.16.00476

Sakschewski, B., Von Bloh, W., Boit, A., Poorter, L., Peña-Claros, M., Heinke, J., et al. (2016). Resilience of Amazon Forests emerges from plant trait diversity. *Nat. Clim Chang.* 6, 1032–1036. doi: 10.1038/nclimate3109

Salazar, D., Lokvam, J., Mesones, I., Pilco, M. V., Zuñiga, J. M. A., De Valpine, P., et al. (2018). Origin and maintenance of chemical diversity in a species-rich tropical tree lineage. *Nat. Ecol. Evol.* 2, 983–990. doi: 10.1038/s41559-018-0552-0

Sardans, J., Llusià, J., Niinemets, Ü., Owen, S., and Peñuelas, J. (2010). Foliar mono- and sesquiterpene contents in relation to leaf economic spectrum in native and alien species in oahu (Hawai'i). *J. Chem. Ecol.* 36, 210–226. doi: 10.1007/s10886-010-9744-z

Sarkar, C., Guenther, A. B., Park, J.-H., Seco, R., Alves, E., Batalha, S., et al. (2020). PTR-TOF-MS eddy covariance measurements of isoprene and monoterpene fluxes from an eastern Amazonian rainforest. *Atmos Chem. Phys.* 20, 7179–7191. doi: 10.5194/acp-20-7179-2020

Schmitt, A. U., Ament, F., de Araújo, A. C., Sá, M., and Teixeira, P. (2023). Modeling atmosphere–land interactions at a rainforest site – a case study using Amazon Tall Tower Observatory (ATTO) measurements and reanalysis data. *Atmos Chem. Phys.* 23, 9323–9346. doi: 10.5194/acp-23-9323-2023

Schneider, C. A., Rasband, W. S., and Eliceiri, K. W. (2012). NIH Image to ImageJ: 25 years of image analysis. *Nat. Methods* 9, 671–675. doi: 10.1038/nmeth.2089

Sedio, B. E., Echeverri, J. C. R., Boya, C. A., and Wright, S. J. (2017). Sources of variation in foliar secondary chemistry in a tropical forest tree community. *Ecology* 98, 616–623. doi: 10.1002/ecy.1689

Segrestin, J., Sartori, K., Navas, M. L., Kattge, J., Díaz, S., and Garnier, E. (2021). PhenoSpace: A Shiny application to visualize trait data in the phenotypic space of the global spectrum of plant form and function. *Ecol. Evol.* 11, 1526–1534. doi: 10.1002/ece3.6928

Sharkey, T. D., Gray, D. W., Pell, H. K., Breneman, S. R., and Topper, L. (2013). Isoprene synthase genes form a monophyletic clade of acyclic terpene synthases in the TPS-B terpene synthase family. *Evol. (N Y)* 67, 1026–1040. doi: 10.1111/evo.12013

Sharkey, T. D., and Monson, R. K. (2017). Isoprene research – 60 years later, the biology is still enigmatic. *Plant Cell Environ.* 40, 1671–1678. doi: 10.1111/pce.12930

Sindelarova, K., Granier, C., Bouarar, I., Guenther, A., Tilmes, S., Stavrakou, T., et al. (2014). Global data set of biogenic VOC emissions calculated by the MEGAN model over the last 30 years. *Atmos Chem. Phys.* 14, 9317–9341. doi: 10.5194/acp-14-9317-2014

Singsaas, E. L., Lerdau, M., Winter, K., and Sharkey, T. D. (1997). Plant Physiology. 115 (4), 1413–1420.

Slot, M., and Winter, K. (2017). *In situ* temperature response of photosynthesis of 42 tree and liana species in the canopy of two Panamanian lowland tropical forests with contrasting rainfall regimes. *New Phytol.* 214, 1303–1117. doi: 10.1111/nph.14469

Srikanth, P., Maxton, A., Masih, S. A., Sofo, A., and Khan, N. A. (2024). Isoprene: an antioxidant to guard plants against stress. *Int. J. Plant Biol.* 15, 161–174. doi: 10.3390/ijpb15010013

Sun, L., He, Y., Cao, M., Wang, X., Zhou, X., Yang, J., et al. (2024). Tree phytochemical diversity and herbivory are higher in the tropics. *Nat. Ecol. Evol.* 2024, 1–11. doi: 10.1038/s41559-024-02444-2

Taylor, T. C., McMahon, S. M., Smith, M. N., Boyle, B., Violle, C., van Haren, J., et al. (2018). Isoprene emission structures tropical tree biogeography and community assembly responses to climate. *New Phytol.* 220, 435–446. doi: 10.1111/nph.15304

Taylor, T. C., Wisniewski, W. T., Alves, E. G., Oliveira Junior, R. C., and Saleska, S. R. (2021). A new field instrument for leaf volatiles reveals an unexpected vertical profile of isoprenoid emission capacities in a tropical forest. *Front. Forests Global Change* 4. doi: 10.3389/ffgc.2021.668228

ter Steege, H., Poorter, L., Aguirre-Gutiérrez, J., Fortunel, C., Magnusson, W. E., Phillips, O. L., et al. (2025). Functional composition of the Amazonian tree flora and forests. *Commun. Biol.* 8, 1–17. doi: 10.1038/s42003-025-07768-8

Thulasiram, H. V., Erickson, H. K., and Poulter, C. D. (2007). Chimeras of two isoprenoid synthases catalyze all four coupling reactions in isoprenoid biosynthesis. *Sci. (1979)* 316, 73–76. doi: 10.1126/science.1137786

Ton, J., D'Alessandro, M., Jourdie, V., Jakab, G., Karlen, D., Held, M., et al. (2006). Priming by airborne signals boosts direct and indirect resistance in maize. *Plant J.* 49, 16–26. doi: 10.1111/j.1365-313X.2006.02935.x

Valladares, F., Wright, S. J., Lasso, E., Kitajima, K., and Pearcy, R. W. (2000). Plastic phenotypic response to light of 16 congeneric shrubs from a Panamanian rainforest. *Ecology* 81, 1925–1936. doi: 10.1890/0012-9658(2000)081[1925:PPRTLO]2.0.CO;2

Velikova, V. (2008). Isoprene as a tool for plant protection against abiotic stresses. *J. Plant Interact.* 3, 1–15. doi: 10.1080/17429140701858327

Velikova, V., Várkonyi, Z., Szabó, M., Maslenkova, L., Nogues, I., Kovács, L., et al. (2011). Increased thermostability of thylakoid membranes in isoprene-emitting leaves probed with three biophysical techniques. *Plant Physiol.* 157, 905–916. doi: 10.1104/pp.111.182519

Violle, C., Navas, M.-L., Vile, D., Kazakou, E., Fortunel, C., Hummel, I., et al. (2007). Let the concept of trait be functional! *Oikos* 116, 882–892. doi: 10.1111/j.2007.0030-1299.15559.x

Visakorpi, K., Gripenberg, S., Malhi, Y., Bolas, C., Oliveras, I., Harris, N., et al. (2018). Small-scale indirect plant responses to insect herbivory could have major impacts on canopy photosynthesis and isoprene emission. *New Phytol.* 220, 799–810. doi: 10.1111/nph.15338

Vleminckx, J., Fortunel, C., Valverde-Barrantes, O., Timothy Paine, C. E., Engel, J., Petronelli, P., et al. (2021). Resolving whole-plant economics from leaf, stem and root traits of 1467 Amazonian tree species. *Oikos* 130, 1193–1208. doi: 10.1111/oik.08284

Vleminckx, J., Salazar, D., Fortunel, C., Mesones, I., Dávila, N., Lokvam, J., et al. (2018). Divergent secondary metabolites and habitat filtering both contribute to tree species coexistence in the Peruvian Amazon. *Front. Plant Sci.* 9. doi: 10.3389/fpls.2018.00836

Weraduwage, S. M., Whitten, D., Kulke, M., Sahu, A., Vermaas, J. V., and Sharkey, T. D. (2024). The isoprene-responsive phosphoproteome provides new insights into the putative signalling pathways and novel roles of isoprene. *Plant Cell Environ.* 47, 1099–1117. doi: 10.1111/pce.14776

Wickham, H. (2016). *ggplot2: elegant graphics for data analysis* (New York, NY, USA: Springer-Verlag).

Wright, I. J., Reich, P. B., Westoby, M., Ackerly, D. D., Baruch, Z., Bongers, F., et al. (2004). The worldwide leaf economics spectrum. *Nature* 428, 821–827. doi: 10.1038/nature02403

Xiao, Y., Wang, Q., Erb, M., Turlings, T. C. J., Ge, L., Hu, L., et al. (2012). Specific herbivore-induced volatiles defend plants and determine insect community composition in the field. *Ecol. Lett.* 15, 1130–1139. doi: 10.1111/j.1461-0248.2012.01835.x

Xu, L., Kollman, M. S., Song, C., Shilling, J. E., and Ng, N. L. (2014). Effects of NOx on the volatility of secondary organic aerosol from isoprene photooxidation. *Environ. Sci. Technol.* 48, 2253–2262. doi: 10.1021/es404842g

Yáñez-Serrano, A. M., Bourtsoukidis, E., Alves, E. G., Bauwens, M., Stavrakou, T., Llusià, J., et al. (2020). Amazonian biogenic volatile organic compounds under global change. *Glob. Chang. Biol.* 26, 4722–4751. doi: 10.1111/gcb.15185

Yáñez-Serrano, A. M., Christine Nölscher, A., Bourtsoukidis, E., Gomes Alves, E., Ganzeveld, L., Bonn, B., et al. (2018). Monoterpene chemical speciation in a tropical rainforest:variation with season, height, and time of day at the Amazon Tall Tower Observatory (ATTO). *Atmos Chem. Phys.* 18, 3403–3418. doi: 10.5194/acp-18-3403-2018

Yáñez-Serrano, A. M., Nölscher, A. C., Williams, J., Wolff, S., Alves, E., Martins, G. A., et al. (2015). Diel and seasonal changes of biogenic volatile organic compounds within and above an Amazonian rainforest. *Atmos Chem. Phys.* 15, 3359–3378. doi: 10.5194/acp-15-3359-2015

Yuan, Y., Sun, Z., Kännaste, A., Guo, M., Zhou, G., and Niinemets, Ü. (2020). Isoprenoid and aromatic compound emissions in relation to leaf structure, plant growth form and species ecology in 45 East-Asian urban subtropical woody species. *Urban For Urban Green* 53. doi: 10.1016/j.ufug.2020.126705

Zanne, A., Lopez-Gonzalez, G., Coomes, D., Ilic, J., Jansen, S., Lewis, S., et al. (2009). *Global wood density database. Data from: Towards a worldwide wood economics spectrum. Dryad Digital Repository.* doi: 10.5061/dryad.234

Zeng, J., Zhang, Y., Pang, W., Ran, H., Guo, H., Song, W., et al. (2024). Optimizing *in-situ* measurement of representative BVOC emission factors considering intraspecific variability. *Geophys. Res. Lett.* 51, e2024GL108870. doi: 10.1029/2024GL108870

Zhao, L., Chang, W. C., Xiao, Y., Liu, H. W., and Liu, P. (2013). Methylerythritol phosphate pathway of isoprenoid biosynthesis. *Annu. Rev. Biochem.* 82, 497–530. doi: 10.1146/annurev-biochem-052010-100934

Zuo, Z., Weraduwage, S. M., Lantz, A. T., Sanchez, L. M., Weise, S. E., Wang, J., et al. (2019). Isoprene acts as a signaling molecule in gene networks important for stress responses and plant growth. *Plant Physiol.* 180, 124–152. doi: 10.1104/pp.18.01391